

**ROBOTIC CONTOUR TRACKING WITH ADAPTIVE  
FEEDFORWARD CONTROL BY FUZZY ONLINE TUNING**

by  
**Beste BAHÇECİ**

**Submitted to the Graduate School of Engineering and Natural Sciences  
in partial fulfillment of the requirements for the degree of Master of  
Science**

**Sabanci University  
August 2013**

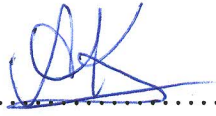
**ROBOTIC CONTOUR TRACKING WITH ADAPTIVE  
FEEDFORWARD CONTROL BY FUZZY ONLINE TUNING**

APPROVED BY:

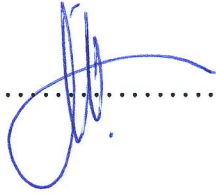
Assoc. Prof. Dr. Kemalettin ERBATUR  
(Thesis Advisor)

  
.....

Assoc. Prof. Dr. Ali KOŞAR

  
.....

Assoc. Prof. Dr. Mahmut F. AKŞİT

  
.....

Assoc. Prof. Dr. Albert LEVİ

  
.....

Asst. Prof. Dr. Alpay TARALP

  
.....

DATE OF APPROVAL:

13<sup>th</sup> of August, 2013.

.....

© Beste BAHÇECİ  
2013

All Rights Reserved

ROBOTIC CONTOUR TRACKING WITH ADAPTIVE FEEDFORWARD  
CONTROL BY FUZZY ONLINE TUNING

Beste BAHÇECİ

Mechatronics Engineering, M.Sc Thesis, 2013

Thesis Supervisor: Assoc. Prof. Dr. Kemalettin ERBATUR

Keywords: Contour tracking, force control, fuzzy tuning, feedforward control

**ABSTRACT**

Industrial robots have great importance in manufacturing. Typical uses of the robots are welding, painting, deburring, grinding, polishing and shape recovery. Most of these tasks such as grinding, deburring need force control to achieve high performance. These tasks involve contour following.

Contour following is a challenging task because in many of applications the geometry physical of the targeted contour are unknown. In addition to that, achieving tasks as polishing, grinding and deburring requires small force and velocity tracking errors. In order to accomplish these tasks, disturbances have to be taken account.

In this thesis the aim is to achieve contour tracking with using fuzzy online tuning. The fuzzy method is proposed in this thesis to adjust a feedforward force control parameter. In this technique, the varying feedforward control parameter compensates for disturbance effects.

The method employs the chattering of control signal and the normal force and tangential velocity errors to adjust the control term. Simulations with the model of a direct drive planar elbow manipulator are used to last proposed technique.

# ROBOTİK KONTÜR İZLEME İÇİN BULANIK ÇEVİRİMİÇİ AYARLAMA İLE UYARLAMALI İLERİ BESLEME KONTROLÜ

Beste BAHÇECİ

Mekatronik Mühendisliği Programı, Master Tezi, 2013

Tez Danışmanı: Doç. Dr. Kemalettin ERBATUR

Anahtar Kelimeler:

## ÖZET

Endüstriyel robotların üretimdeki yeri çok büyüktür. Bu robotların genel kullanım araçları; kaynaklama, boyama, taşlama, zımparalama, cilalama ve şekil kurtarmadır. Bu çalışma alanlarının çoğu yüksek performans elde edebilmek için kuvvet kontrolüne ihtiyaç duymaktadır. Kuvvet kontrolüne ihtiyaç duyan alanların bazıları; taşlama ve zımparalamadır. Ek olarak bu çalışma alanları kontür izlemeyi de içerir.

Kontür izleme yüksek miktarda efor talep eden, komplike bir işlemdir, çünkü birçok uygulamada izlenmesi gereken kontürün fiziksel özellikleri ve geometrisi belirsizdir. Buna ek olarak cilalama, taşlama ve zımparalama gibi işlemlerin başarıyla tamamlanabilmesi için eser miktarda kuvvet ve hız hatası elde etmek gereklidir. Ayrıca bu işlemlerin başarıyla uygulanabilmesi için çevresel bozucu etkilerin de dikkate alınması gerekmektedir.

Bu tezin amacı bulanık çevrimiçi ayarlama kullanarak kontür izleme işlemini başarıyla gerçekleştirmektir. İleri beslemeli kuvvet kontrolü değişkenini ayarlamak için kullanılan bulanık method, bu tezde anlatılmıştır. Bu teknikte, değişken ileri besleme kontrol katsayısı çevresel bozucu etkileri kompanse eder.

Bu method, kontrol signali çatırdamasını ve normal kuvvet ve teğetsel hız hatalarını kullanarak, kontrol katsayısını düzenler. Doğrusal işletme düzenli düzlemsel dirsek manipülatörü örnek alınarak yapılan simulasyonlar kullanılarak bahsedilen tekniğin uygulanmıştır.

*To my friends and family*

## ACKNOWLEDGEMENTS

I would like to express my deepest gratitude to my MS thesis supervisor, Assoc. Prof. Dr. Kemalettin ERBATUR. His endless support towards overcoming obstacles I faced, paved the way through this accomplishment. His encouraging guidance and warm attitude made this thesis possible. During thesis writing period, he has been extraordinarily tolerant and supportive. I will always be indebted to him for shaping my future in academic life.

Besides my advisor, I would like to thank the rest of my thesis committee: Assoc. Prof. Dr. Ali KOŞAR, Assoc. Prof. Dr. Mahmut F. AKŞİT, Assoc. Prof. Dr. Albert LEVİ and Assist. Prof. Dr. Alpay TARALP for their insightful comments.

I am indebted to my friends and colleagues for their support and for providing a funny environment. I am especially grateful to Ahmet Fatih TABAK, Ebru UYSAL, Emre ÖZEREN, Eray BARAN, Evrim KURTOĞLU, Hadi Çağdaş ERK, İlker SEVGEN, Kübra AK, Merve SAYAR, Mine SARAÇ, Soner ULUN and many other friends in Sabancı University Mechatronics laboratories. I am also grateful for all times we spent together with Gökçe Firuze AVCI, I hope she is peaceful wherever she is.

Special thanks to Zahide KAMIŞLI, for her advises from my childhood. Her effect on my character cannot be denied. Her influence made me a better person. She will always be a role model for me.

Lastly, I wish to thank my family, Hakan BAHÇECİ, Özdem BAHÇECİ, my brother Egemen BAHÇECİ, my grandparents Ülker BAHÇECİ and Tahir BAHÇECİ. They raised me, supported me, taught me and loved me. I owe greatest debt to them.

ROBOTIC CONTOUR TRACKING WITH ADAPTIVE FEEDFORWARD  
CONTROL BY FUZZY ONLINE TUNING

**TABLE OF CONTENTS**

ABSTRACT.....	iv
ÖZET .....	v
ACKNOWLEDGMENTS .....	vii
TABLE OF CONTENTS.....	viii
LIST OF FIGURES .....	x
LIST OF TABLES.....	xi
LIST OF SYMBOLS .....	xii
LIST OF ABBREVIATIONS.....	xv
1. INTRODUCTION .....	1
2. LITARATURE REVIEW .....	3
2.1. Fuzzy Logic Systems .....	3
2.2. Contour Tracking.....	12
2.3. Feed-forward Control .....	17
3. PLANT, FORCE CONTROL AND CONTOUR TRACKING.....	21
3.1. Fuzzy.....	21
3.2. Force Control and Contour Tracking Algorithm .....	24
4. FUZZY PARAMETER ADJUSTMENT .....	34
5. CONCLUSSION .....	48
6. REFERENCES .....	49

## LIST OF FIGURES

Figure 2.1.1: Deburring Process.....	4
Figure 2.1.2: Model of contact between end effector and environment.....	5
Figure 2.1.3: Fuzzy-Neural Network.....	6
Figure 2.1.4: Membership function of fuzzy rule.....	7
Figure 2.1.5: Contour tracking task.....	8
Figure 2.1.6: Figure of a two link manipulator.....	9
Figure 2.1.7: Complete fuzzy rule base.....	10
Figure 2.1.8: Phases of swing up and handstand control process.....	12
Figure 2.2.1: Displacement along contour.....	13
Figure 2.2.2: Geometry of tool against an edge.....	14
Figure 2.2.3: Slot following in two dimensions.....	15
Figure 2.2.4: SCARA manipulator.....	16
Figure 2.2.5: Toshiba direct drive arm.....	17
Figure 2.3.1: Feedback-feedforward control system.....	18
Figure 2.3.2: PD control with computed feedforward.....	19
Figure 2.3.3: Single dof robot arm model.....	20
Figure 2.3.4: Prototype robot manipulator.....	20
Figure 3.1.1: SCARA type robot arm and link models.....	23
Figure 3.1.2: Robot joint angle descriptions and length parameters.....	23
Figure 3.2.1: Wall and end effector positions.....	29
Figure 3.2.2: Actual and reference normal force.....	30
Figure 3.2.3: Actual and reference y-axis position.....	31
Figure 3.2.4: Shoulder and elbow positions.....	32
Figure 3.2.5: Shoulder and elbow torques.....	33
Figure 4.1: Trapezoid functions for $\Gamma$ .....	37
Figure 4.2: Trapezoid functions for $E$ .....	37
Figure 4.3: Wall and end effector positions.....	40
Figure 4.4: Actual and reference y-axis position and actual and reference normal force.....	41
Figure 4.5: Shoulder and elbow positions in polar coordinates.....	42
Figure 4.6: Shoulder torque and chattering.....	43

Figure 4.7: Elbow torque and chattering.....	44
Figure 4.8: Feedforward gain parameters.....	45
Figure 4.9: Error of y-axis positions for two simulations .....	46
Figure 4.10: Error of normal force for two simulations .....	47

## LIST OF TABLES

Table 3.1.1 : Robot Parameters.....	24
Table 3.2.1 : Controller Parameters.....	25
Table 3.2.2 : Force, velocity control parameters.....	27
Table 3.2.3 : Wall parameters.....	28
Table 4.1 : Fuzzy rule parameters.....	37
Table 4.2 : Fuzzy rule values.....	37
Table 4.3 : Corner values.....	37

## LIST OF SYMBOLS

$a_{wall}$	:	Wall's position line parameter
$B_1$	:	Viscous coefficient for base joint
$B_2$	:	Viscous coefficient for elbow joint
$b_{wall}$	:	Wall's position line parameter
$C$	:	Centripetal and Coriolis effect matrix
$c_1$	:	Center of mass point for link 1
$c_2$	:	Center of mass point for link 2
$c_{wall}$	:	Wall's position line parameter
$D$	:	Manipulator inertia matrix
$d_{wall}$	:	Wall's position line parameter
$E$	:	Error matrix
$E_{Big}$	:	Corner value for trapezoid function $\mu_{Big E}$
$e_F$	:	Error for normal force
$E_{Small}$	:	Corner value for trapezoid function $\mu_{Small E}$
$e_V$	:	Error for tangential velocity
$F_b$	:	Wall damper force
$F_{c1}$	:	Coulomb friction torque for base joint
$F_{c2}$	:	Coulomb friction torque for elbow joint
$F_{e_x}$	:	Force on tool tip in x axis direction
$F_{e_y}$	:	Force on tool tip in y axis direction
$F_k$	:	Wall spring force
$F_N$	:	Actual normal force
$I_1$	:	Inertia of link 1
$I_2$	:	Inertia of link 2
$J_1$	:	Rotor inertia value for base joint
$J_2$	:	Rotor inertia value for elbow joint

$J_M$	:	Jacobian of the manipulator
$k_{b-wall}$	:	Wall's damper constant
$K_D$	:	Derivative control coefficient matrix
$k_{D_f}$	:	Derivative control coefficient for normal force
$k_{D_v}$	:	Derivative control coefficient for tangential velocity
$k_F$	:	Feedforward coefficient of normal force
$K_I$	:	Integral control coefficient matrix
$k_{I_f}$	:	Integral control coefficient for normal force
$k_{I_v}$	:	Integral control coefficient for tangential velocity
$K_P$	:	Proportional control coefficient matrix
$k_{P_f}$	:	Proportional control coefficient for normal force
$k_{P_v}$	:	Proportional control coefficient for tangential velocity
$K_R$	:	Feedforward control coefficient matrix
$k_V$	:	Feedforward coefficient of tangential velocity
$k_{wall}$	:	Wall's spring constant
$l_1$	:	Length for link 1
$l_2$	:	Length for link 2
$l_{c1}$	:	Distance of joint center of mass for link 1
$l_{c2}$	:	Distance of joint center of mass for link 2
$m_1$	:	Mass for link 1
$m_2$	:	Mass for link 2
$q_1$	:	Joint angular position for base joint
$q_2$	:	Joint angular position for elbow joint
$\dot{q}_1$	:	Joint angular velocity for base joint
$\dot{q}_2$	:	Joint angular velocity for elbow joint
$\ddot{q}_1$	:	Joint angular acceleration for base joint
$\ddot{q}_2$	:	Joint angular acceleration for elbow joint
$R$	:	Reference vector

$ref_n$	:	Reference normal force
$ref_t$	:	Reference tangential velocity
$U_{PID}$	:	PID control output matrix
$U_{PID_F}$	:	PID control output for normal force
$U_{PID_v}$	:	PID control output for tangential velocity
$V_{e_x}$	:	Manipulator end effector velocity on x axis
$V_{e_y}$	:	Manipulator end effector velocity on y axis
$x_e$	:	Manipulator end effector position on x axis
$x_{wall}$	:	Wall's Cartesian coordinate on x axis
$y_e$	:	Manipulator end effector position on y axis
$y_{wall}$	:	Wall's Cartesian coordinate on y axis
$\tau_1$	:	Joint actuation torque for base joint
$\tau_2$	:	Joint actuation torque for elbow joint
$\Gamma$	:	Chattering variable
$\Gamma_1$	:	Chattering variable for base joint
$\Gamma_2$	:	Chattering variable for elbow joint
$\Gamma_{Big}$	:	Corner value for trapezoid function $\mu_{Big \Gamma}$
$\Gamma_{Small}$	:	Corner value for trapezoid function $\mu_{Small \Gamma}$
$\Delta K_{R BB}$	:	Fuzzy rule parameter for big chattering and big error
$\Delta K_{R BS}$	:	Fuzzy rule parameter for small chattering and big error
$\Delta K_{R SB}$	:	Fuzzy rule parameter for big chattering and small error
$\Delta K_{R SS}$	:	Fuzzy rule parameter for small chattering and small error
$\mu_{Big E}$	:	Trapezoid function for big error
$\mu_{Big \Gamma}$	:	Trapezoid function for big chattering
$\mu_{Small E}$	:	Trapezoid function for small error
$\mu_{Small \Gamma}$	:	Trapezoid function for small chattering

## **LIST OF ABBREVIATIONS**

DOF	:	Degrees of Freedom
DC	:	Direct Current
PD	:	Proportional Derivative
PID	:	Proportional Integral Derivative
Val-II	:	Variable Assembly Language II
DSP	:	Digital Signal Processors
CAD	:	Computer Aided Design
COM	:	Center of Mass

## **Chapter 1**

### **1. INTRODUCTION**

An industrial robot is a manipulator which is reprogrammable by computer interface, automatically controlled and multi-purpose. They typically have three or more degrees of freedom (DOF) [1]. Single or two DOF manipulators are mostly used for research purposes due to their simplicity. Industrial robots are employed for a wide range of manufacturing: such as grinding [2], deburring [2], polishing [3], painting [4], shape recovery [5], welding [6], assembly [7], pick and place [8] and product inspection and testing. Robots provide speed and accuracy, which provide quick production quality of products.

Force control comes into the picture in conjunction specialized tasks requiring production of smooth shaped surfaces and parts. Grinding, deburring, polishing and shape recovery are some of these tasks. These tasks are expected to meet not only predefined dimensions but also desired surface quality. Human force can accomplish these qualities, however, speed and perfection of human labor is lower than robotic manufacturing. Contour tracking poses a particularly challenging task [9]. Environmental conditions and disturbances can affect contour tracking results. Elasticity of joints, joint frictions, friction with the contact object and unknown geometry of the contact surface are the most common problems.

Feedforward control is a control method which concentrates on the inputs rather than on the outputs to maintain a specified state. It reacts faster than feedback control and it potentially minimizes problems before they occur. This means that disturbances accounted before they can affect the system. Feedforward gains can be computed adaptively. Adaptive

feedforward control is useful in environments where the disturbance is subject to several stimuli.

Fuzzy logic is a form of probabilistic reasoning. It deals with approximating values that are not fixed or exact. In controller design fuzzy logic is used to analyze analog input values that take continuous values between 0 and 1. It is different from classical or digital logic because classical logic works discrete, i.e. the truth values are equal to either 0 or 1. Fuzzy online tuning is useful with uncertainties and different operating conditions. It handles adaptation, tuning and scheduling of the parameters of control systems for desired performance of robustness. This method can use two or more variables to tune controller parameters, in our case fuzzy online tuning is used to modify the feedforward control term, in a contour tracking application.

In contour tracking applications, considering that the robot manipulator is in contact with a rigid object, chattering in control signal is supposed to occur because of contact forces. In order to achieve a smooth tracking chattering must be lessened. Measurement of chattering in control signal is proposed in this thesis to tune the feedforward control parameter. Additionally, errors in tangential velocity and normal force must be small. Therefore, these errors are used for the tuning. The tuning algorithm includes chattering in the control signal and normal force and tangential velocity errors.

In the literature, contour tracking tasks are studied with various controllers. Feedforward control is one of them. Adaptive feedforward control is mentioned in several studies too. Fuzzy parameter adjustment is not used for feedforward gain adjustment in these studies. In this thesis adaptive feedforward control with a fuzzy parameter adjustment technique is proposed for contour tracking tasks to reduce errors in tangential and normal directions.

This thesis is organized as follows. Chapter 2 presents a literature reviews on fuzzy logic, force control and contour tracking. The model of the robot arm used as a simulation test bed as described and the contour tracking algorithm is introduced in Chapter 3. Chapter 4 is devoted to the proposed fuzzy parameter adjustment method. The conclusion is presented lastly.

## **Chapter 2**

### **2. LITARATURE REVIEW**

In order to have satisfactory control performance in contour tracking applications robot joint friction effects should be taken into account. In the literature there are a number of reports on this subject. In first part of this section, firstly, fuzzy logic systems and fuzzy control are discussed, and then contour tracking and lastly feedforward control are reviewed.

#### **2.1. Fuzzy Logic Systems**

In a study by Liu [10], a technique with fuzzy control is proposed for robotic deburring. The deburring process is illustrated in Figure 2.1.1, where  $n$  stands for the normal direction,  $t$  denotes tangential direction and  $v$  represents velocity. The fuzzy control algorithm is used to decrease normal and tangential velocity errors. Force feedback is employed. This technique is useful for the systems with positional inaccuracies and unknown burr size. Experimental results show that this technique is successful at decreasing the position error.

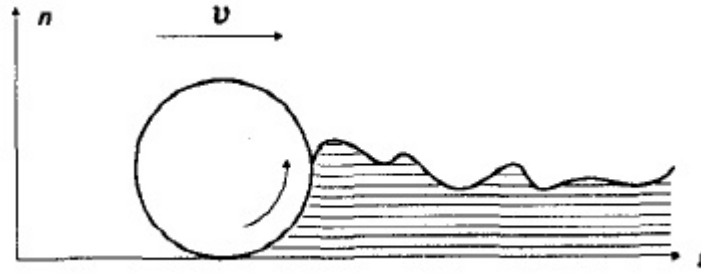


Figure 2.1.1: Deburring Process [10]

Another important force control study [11] employs sliding mode fuzzy control. The authors compare fuzzy control with sliding mode control. They show that a fuzzy controller with boundary layer provides adaptive tracking quality under changing plant parameters. And a well designed fuzzy controller with boundary layer gives better results than sliding mode controller with boundary layer [11].

A completely fuzzified adaptive control scheme is developed for single degree of freedom mechanisms whose end effector is in contact with their environment (Figure 2.1.2). Here  $m_1$  is mass of the manipulator,  $v_1$  is its velocity,  $r$  is radius of the reduction gear,  $K_s$  represents the stiffness coefficient of the force sensor,  $b_s$  is the damping coefficient of the force sensor,  $x_1$ ,  $x_2$  and  $x_3$  are positions of the manipulator, the end effector and the work piece, respectively. Also,  $m_2$  denotes the mass of end effector and  $K_e$  represents the stiffness coefficient of environment.  $T_e$  and  $w$  stand for the torque and the angular velocity of the reduction gear, respectively. The force control loop has adaptive fuzzy force controller with a subordinated fuzzy velocity controller embedded in it. The algorithm has a nonintegral behavior and it is active only during system transitions. Simulations are done with different stiffness values of the environment. The error between the model and the system output can be maintained in desired limits by using a second order reference input [12].

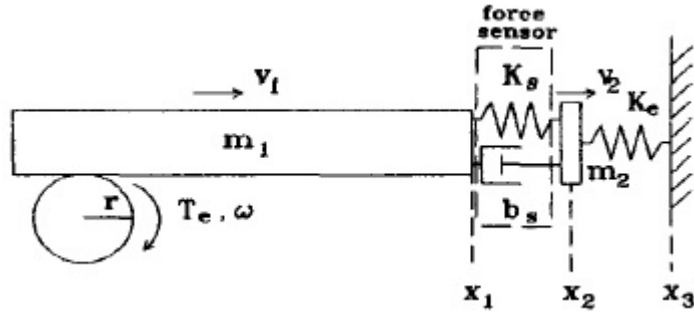


Figure 2.1.2: Model of contact between end effector and environment [12]

Fuzzy logic systems have the ability to deal with human knowledge and neural networks have the ability to learn from experiments. The two methods can be used together to compensate for their weak points. A fuzzy-neural controller is reported for robot manipulator contact force control to an unknown environment [13]. The fuzzy neural network is shown in the Figure 2.1.3, where  $M_o$  is the momentum of the robot manipulator,  $E$  is the error between the desired force and the applied force,  $\Sigma$  stands for the sum of the inputs, and  $\Pi$  depicts the product of inputs. The fuzzifier layer has 10, the rule layer has 17 and the defuzzifier layer has 2 neurons,  $f_G$  and  $f_s$  are activation functions, and  $U$  represents the force command to the robot manipulator. The error between the desired force and the measured force and the momentum of robot manipulator are used as inputs to the controller. The controller is adjusted online by a back propagation algorithm and the approach velocity is controlled to be slow to reduce initial applied force. Simulations show that contact force is controlled efficiently [13, 14].

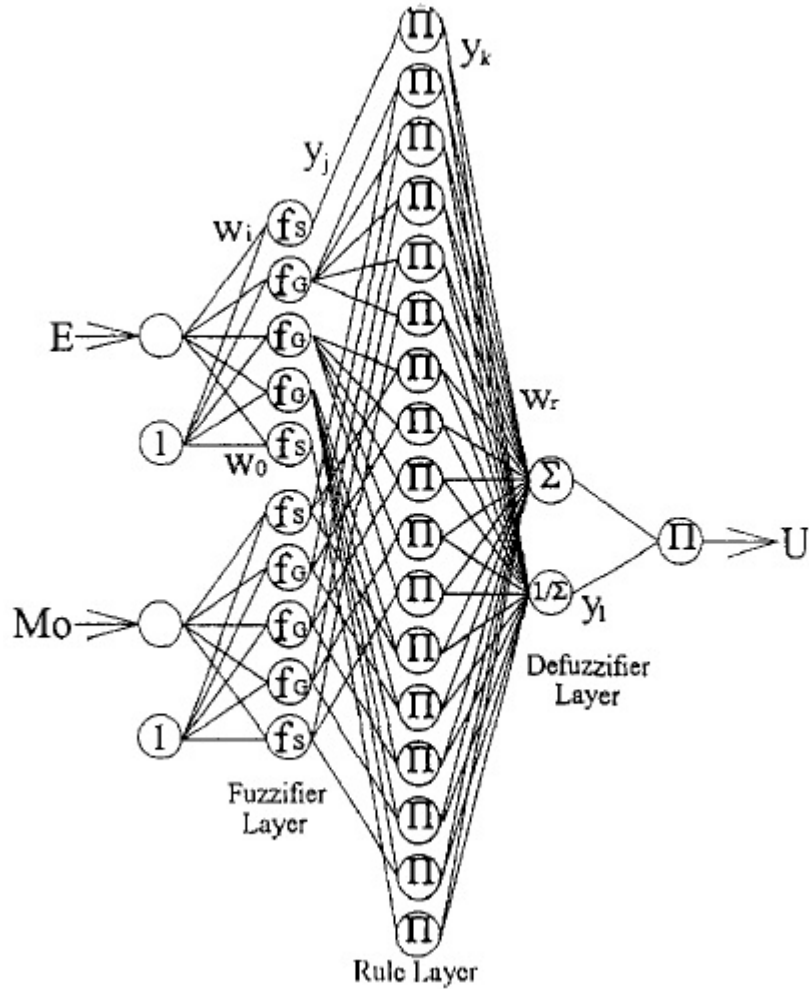
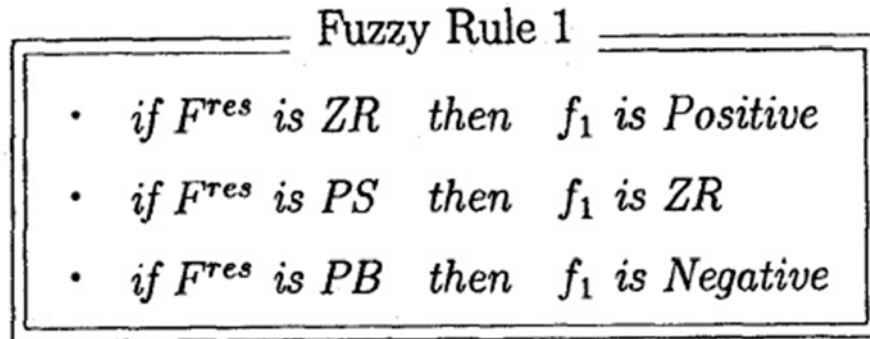


Figure 2.1.3: Fuzzy-Neural Network [14]

In some works, position and force control techniques are unified. In this scheme, these two methods and an intermediary control are realized through one controller. The observed disturbance is used to increase the robustness of the system. The observer makes it possible to estimate the parameters of the environment. A force controller based on the impedance control idea uses the estimated parameters. Switching between control-laws is carried out by using fuzzy logic. The fuzzy rule base studied by Shibata and Murakami [15] is shown in Figure 2.1.4, where  $F^{res}$  represents the reaction force from the object which end effector is in contact with, and  $f_1$  means a fuzzy rule 1. The resulting system is used for touching and pushing tasks. Results are demonstrated by simulations and experiments and one can see that switching between control laws is quick and smooth. Also the resulting control law is stable [15].



**ZR : Zero**

**PS : Positive Small**

**PB : Positive Big**

Figure 2.1.4: Membership function of fuzzy rule [15]

Nonlinear friction compensation is an area where fuzzy logic used extensively. In the work by Teeter and Chow [16] friction compensation of a DC motor is carried out via fuzzy logic. In [16], the authors used a single fuzzy rule to compensate the nonlinearity of the physical system. Compared with typical fuzzy logic, this method has fewer adjustable parameters and requires a less accurate mathematical model. The resulting model improves the performance of the DC-motor system. This method can be useful in systems where an accurate mathematical modeling is not feasible [16].

Adaptive fuzzy hybrid force-position control is used for achieving contour tracking tasks in the lack of knowledge of exact geometric shape and manipulator dynamics. Figure 2.1.5 shows contour a tracking task. The control algorithm can adaptively update fuzzy control rules and the position trajectory command. Stability of the system is global and tracking errors converge to zero. This control algorithm is applied to a five degrees-of-freedom manipulator and a quick algorithmic convergence is observed [2].

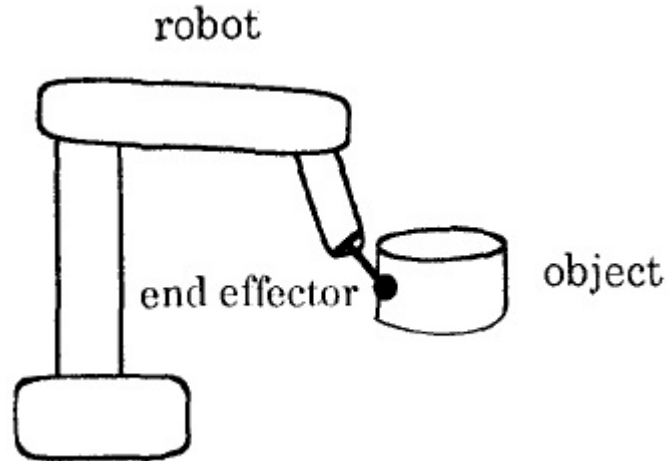


Figure 2.1.5: Contour tracking task [2]

Another neuro-fuzzy controller is proposed in [17] by Kiguchi and Fukuda. The controller is designed to compensate for friction for a position-force hybrid controlled robot. The controller has a neural division for trajectory control and another component for friction compensation. Weight adjustment is switched between these two parts depending on the current situation. Results show that the Coulomb friction is compensated effectively and the measured trajectory follows desired trajectory accurately.

Another investigation on friction compensation is carried out with a fuzzy adaptive technique incorporated into conventional feedback control. Low speed control of a DC-motor which has both lubricated and dry-joints, is used for experiments. Comparison between this technique and control systems without fuzzy adaptation shows that systems that do not have fuzzy adaptation have large stick slip type oscillations and poor tracking performance. Three different control systems, which are type I system with feedback controller, type II system with first order controller, and type II system with PI controller, are examined. They all alleviate of stick-slip type oscillations and achieve high tracking performance [18].

In another work, a robust fuzzy-neural-network sliding-mode-control system based on computed torque control design for a two axis motion control system was studied by Lin [19]. Fuzzy-neural-network sliding-mode-control system is designed to approximate the equivalent control part of the sliding control law. In this study, two axes are controlled independently. The resulting controller eliminated the need for prior knowledge of the controlled plant. The fuzzy neural network estimates a nonlinear function which contains

the uncertainty of the plant. An adaptive algorithm is proposed to adjust the uncertainty term. Experiments and simulations are done employing contour references. The contributions are the derivation of adaptive learning algorithms based on Lyapunov stability for fuzzy neural networks, the development of a robust-fuzzy-neural-network-sliding-mode-control system that can handle approximation error and disturbance, and a control system that can track different reference contours with robust control performance [19].

[20] is another study on an adaptive neural fuzzy controller by Hung and Na. It proposes that friction and disturbances are highly nonlinear and not easy to model. The work firstly presents a feedback linearization controller for the manipulator trajectory tracking, without success. Then a fuzzy system is added on the original system as a parallel controller. This addition improved the tracking performance. Finally a neural network compensator is added in order to obtain friction and disturbance from experiments on a two link manipulator (Figure 2.1.6). Here,  $l_1$  and  $l_2$  are link lengths.  $l_{c1}$  and  $l_{c2}$  are link center of mass distances.  $m_1$  and  $m_2$  are link masses,  $q_1$  and  $q_2$  are joint positions, and  $I_1$  and  $I_2$  are link inertias. The resulting system is successful in high accuracy position control.

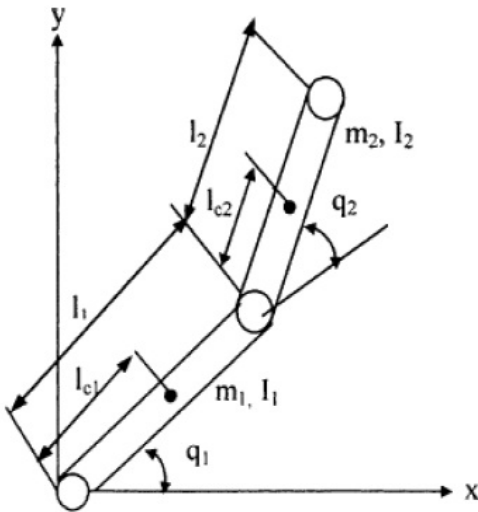


Figure 2.1.6: Figure of a two link manipulator [20]

A study by Wang *et al.* [21] proposes a force control algorithm for the robot manipulators in contact with constraining surfaces of unknown geometry and a certain stiffness error. Real-time adjustment via fuzzy logic is used to obtain an accurate estimate

of the stiffness parameter. The adjustment depends on position feedback and force. The resulting control law is able to minimize the amount of off-line work.

Data mining techniques are useful to develop adaptive fuzzy friction models. In a study by Wang and Wang [22], a data mining algorithm is proposed to extract fuzzy rules (Figure 2.1.7) and to create a static fuzzy friction model.  $B_1^F, B_2^F, B_3^F, B_4^F, B_5^F, A_1^{\dot{x}}, A_2^{\dot{x}}, A_3^{\dot{x}}, A_4^{\dot{x}}$  and  $A_5^{\dot{x}}$  are two sets of linguistic labels. An updating law for fuzzy friction model parameter adjustment is applied based on Lyapunov stability theory. The resulting model is effective and useful to improve control performance.

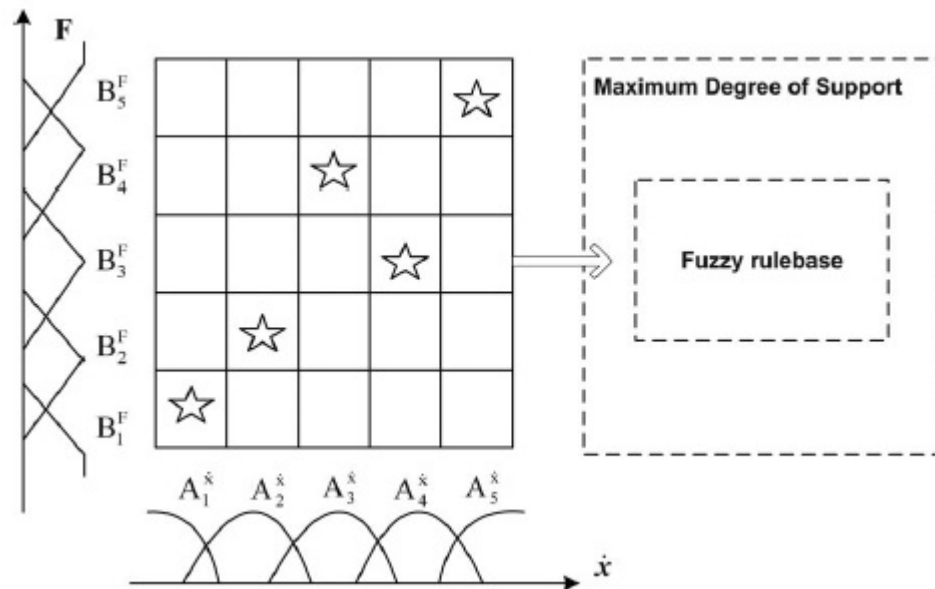


Figure 2.1.7: Complete fuzzy rule base [22]

Force control to handle contact with surfaces can be divided into two subsections: The phase of approaching the work piece and the phase of manipulator contact with the work piece. In the work by Plius *et al.* [23], the first phase is controlled by admittance control and second phase is controlled by integral force control. For scheduling the two controllers, a fuzzy logic scheduling approach is employed. Moreover, this technique is compared to crisp controller switching method. Both free moving pieces and rigidly fixed pieces are used as work pieces. In both cases fuzzy logic based scheduler has better performance than crisp controller switching method.

[24] is a research work on force control with disturbed force sensing. Authors of the study proposed a low-pass filter, to reduce the disturbance, combined with a fuzzy PD control method. The proposed system is compared with traditional PD control. Results show that the PD controller has good dynamic characteristics; however, when the signal is noisy traditional PD control cannot deal with it. A fuzzy PD controller with a low pass filter can obtain successful force output responses. It shows that proposed low pass filter smoothes the noise out and that the fuzzy PD controller achieves better performance and is more efficient than the traditional PD controller.

Online fuzzy tuning method is a technique which is used in a number of control algorithms. Indirect field orientation controlled induction machine drives is an area which is an online fuzzy tuning scheme is used. In [25] by Li *et al.* speed is controlled by a fuzzy controller, detuning of field orientation is corrected by two fuzzy compensations. Detuning effects of indirect field orientation is minimized by these controllers. The overshoot, steady state error, torque disturbance rejection and variable speed tracking performances are improved. An advantage of this control scheme is that this method does not need additional hardware and machine parameter information.

Online fuzzy tuning can also be used for improving sliding mode controller performance. Fuzzy controller dimensions are independent from sliding mode controller complexity. The fuzzy system in [26] by Javaheri and Vossoughi continuously optimizes sliding mode controller gains, i.e. such as hitting control gain, boundary layer thickness, sliding surface slope and intercept. Numbers of fuzzy rules, which are used in the controller, are not restricted with system order and complexity. They are only depending on system outputs. The combined system is robust with high tracking speed and low tracking error and it achieves minimal chattering without increasing system's sensitivity to external disturbances.

A self tuning controller structure simulating the self tuning of an intelligent human controller is designed with fuzzy logic rules [27]. A cart double pendulum system is controlled with swing up control and the control system has fuzzy tuning abilities. Figure 2.1.8 shows four phases of swing up control and handstand control processes of the cart double pendulum. Simultaneously, sensitive and nonsensitive parameters are separated from each other. This separation solves explosion problem in the parameter rules.

Separation of parameters also reduces dimension of the control rule and improves the real time characteristics of the proposed algorithm.

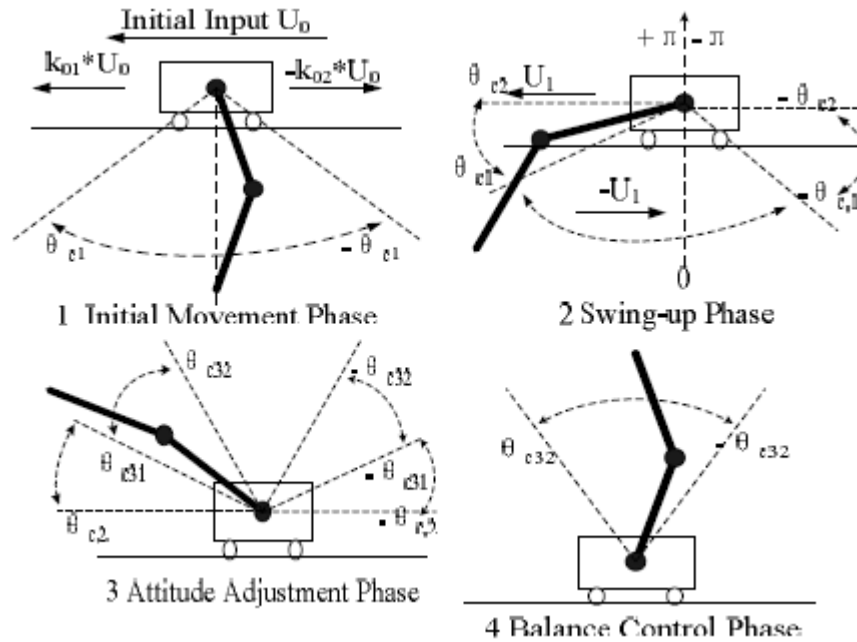


Figure 2.1.8: Phases of swing up and handstand control process [27]

The adaptive controller named in [28] by Truong *et al.* as online tuning modified grey fuzzy proportional integral derivative controller is a combination of a main control unit with an online tuning fuzzy PID unit and an online tuning modified grey predictor. The controller consists of an adaptive PID controller based on online fuzzy neural technique. A smart learning mechanism is implemented on the controller to optimize parameters for error minimization. Simulation results show that resulting system can deal with environments with large perturbations.

## 2.2. Contour Tracking

Shape recovery is the process of finding out the shape information of an object with unknown contour. It can be performed by contour tracking algorithms. Figure 2.2.1 shows displacement along a contour. Usually, force feedback used for this process. In Ahmad and

Lee's work [5], authors discussed about creating an algorithm to follow unknown planar contour with position controlled robot using steady state contact force information: When direct kinematics is used to recover object's shape, there is distortion of the original contour because of the nonlinearities of drive train and lack of knowledge of position of robot tool. The drive train is used to generate a mathematical model of these errors. In addition to that, several compensation strategies are explored by the authors. Results of conducted experiments show that joint compliance is conveniently compensated. This compensation improves the quality of shape recovery.

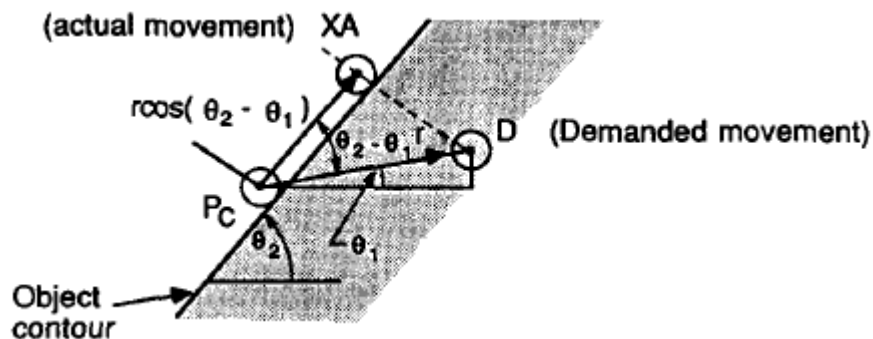


Figure 2.2.1: Displacement along contour [5]

An early research on edge following with industrial manipulators shows that PUMA 560 manipulator can be used in edge following tasks [29]. Figure 2.2.2 illustrates the situation when the robot tool is up against an edge. The PUMA 560 manipulator is employed with an unmodified unimation controller with Val-II language and with a wrist force sensor. Accommodation force control is achieved. The resulting model is fourth order and conditionally stable. Model analysis carried out and experimental results are obtained in Starr's study [29]. Results show that using a simple model is beneficial and response of the model is quite successful.

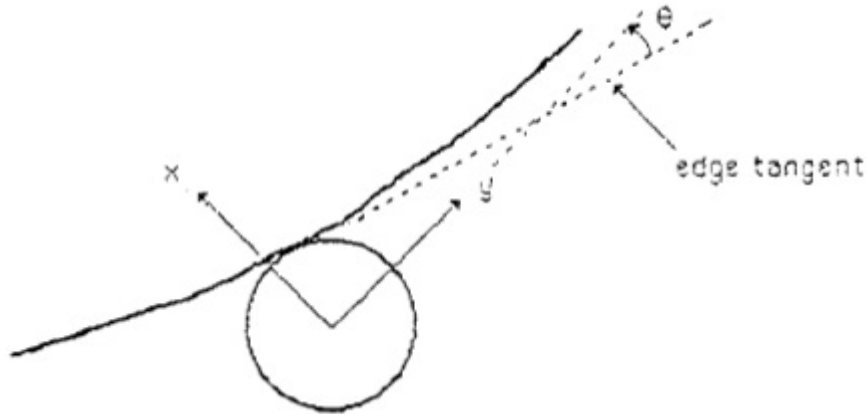


Figure 2.2.2: Geometry of tool against an edge [29]

Another contour following or surface following algorithm is proposed by Bossert *et al.* [30]. In this research hybrid position and force control is used. The proposed algorithm works with unknown surfaces. Their mechanism has a low friction roller at the end of a two link manipulator and the normal force is measured. In addition to normal force, joint angle information is known too. With the knowledge of them, the surface normal direction and position reference are calculated. Algorithm can handle line, concave and convex arc. It performs successfully with different geometries and different force levels, too. It can be also used to exert constant force to known geometries.

The control strategy called dual drive control is a form of hybrid force velocity control. In dual drive control, surface tangent and normal are computed from measured force and velocity. It is useful for tasks that require motion orthogonal to the contact force, such as tracking a surface or turning a crank. These tasks can be performed with a high level planner without continuous intervention. For a two dimensional slot following case, relative velocity and force of a defined point is specified as depicted in Figure 2.2.3:  $P$  is a point which is chosen inside the slot region,  $X$  and  $Y$  are coordinate axes.  $\bar{R}$  is a vector drawn from  $P$  to the end effector.  $\bar{V}$  and  $\bar{F}$  are velocity and force of end effector, respectively. Three dimensional cases can be solved by reducing the number of dimensions and representing the problem with two dimensions. Experiments are done with IBM 7565 manipulator and results show that algorithm is applicable to surface tracking and crank turning [31].

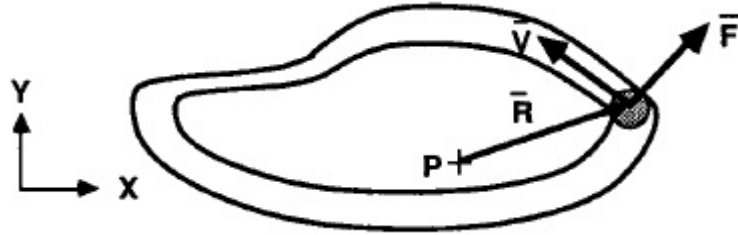


Figure 2.2.3: Slot following in two dimensions [31]

A contour following algorithm which uses hybrid force velocity control is proposed by Yu and Kieffer [9]. The controller allows the end effector tool to follow unknown contours. An empirical force motion model is obtained with experimental measurements. The proposed algorithm is tested for stability and it is proved to be stable. Experiments are conducted with the controller, and it is verified that the tracking performance of tangential velocity and normal forces for various unknown contours of the controller is reliable. To increase controller's tolerance to variations in contact parameters an adaptive control method is developed. This method uses on-line recursive parameter estimation. This update is seen to be effective in experiments.

An extension of the hybrid position force control method, dynamic hybrid control, is proposed by Raibert and Craig [32]. This method needs the knowledge of the manipulator dynamics and constraints on the end effector. However, the object with which the end effector is in contact with, has usually unknown parameters such as size and position. Dynamic hybrid control method with unknown constraint is further investigated to cope with this difficulty. An online estimation algorithm is proposed to predict the local shape of the constraint surface accurately. The estimator uses end effector position and force data. Combination of the estimation algorithm and dynamic hybrid control method is tested on SCARA type manipulator. Experiments show that the combination is successful and it is useful to decrease the amount of data which should be provided for the algorithm.

A comparison between control strategies is presented for the trajectory tracking control of an industrial robot arm by Visioli and Legnani [1]. Controllers that are compared are decentralized controllers like proportional, integral, and derivative action based controllers, sliding mode controllers; and model based controllers such as computed torque controllers and a neural network based controller. Experimental results on a SCARA manipulator (Figure 2.24) with a simple estimated dynamic model shows that decentralized

controllers can be adequate for most of the industrial operations. However, this work suggests that, in order to achieve low tracking errors for high speed operations, neural network based control algorithms are more convenient [1].

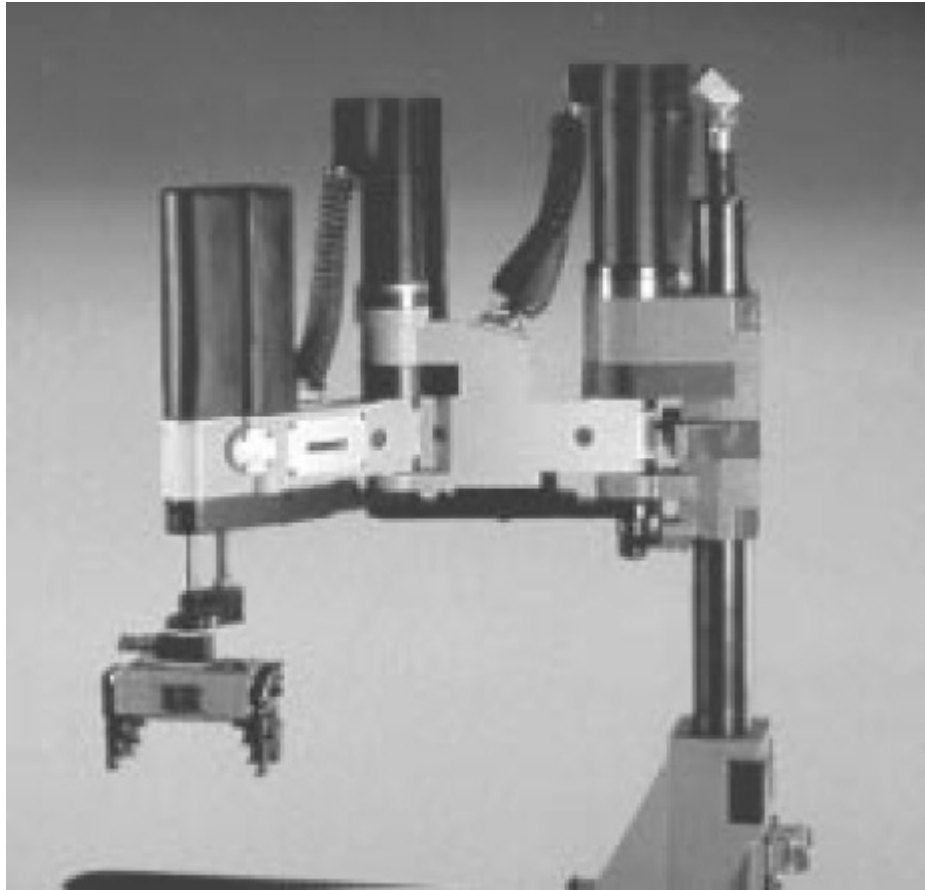


Figure 2.2.4: SCARA manipulator [1]

A new model based adaptive force control algorithm is developed by Whitcomb *et al.* [33]. This new controller provides position and force trajectory tracking of a manipulator which is in contact with a smooth rigid surface. Experiments are carried out with a Toshiba direct drive manipulator (Figure 2.2.5). Stability tests show that this algorithm is stable due to commonly accepted rigid body nonlinear dynamical model for robot arms. Comparison between this new model and a non-model based controller shows that the new method has better performance.

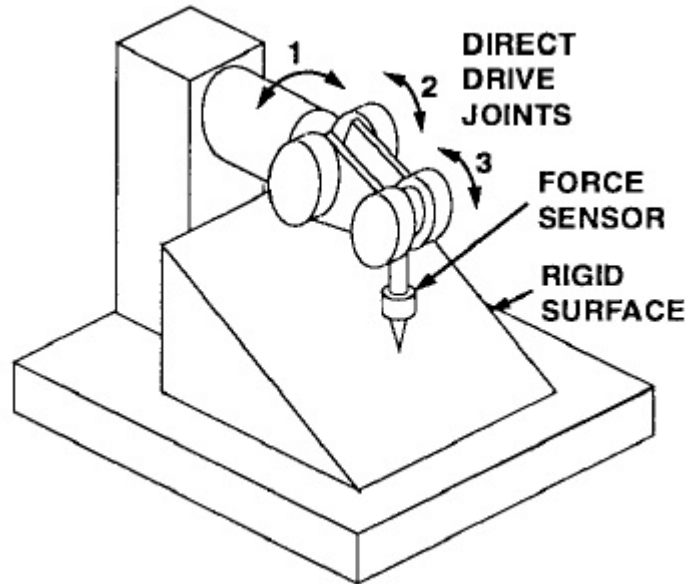


Figure 2.2.5: Toshiba direct drive arm [33]

### 2.3. Feedforward Control

Adaptive feedforward robot control techniques are used in the literature frequently. One of the methods in this field is neural networks. A study by Novakovic [34] presents several concepts, such as combination of input and output functions, input time and varying signal distributions, discrete time domain synthesis and a one step iteration approach. Based on the concepts above, a feedforward neural network is proposed for an adaptive nonlinear robot control. This neural network based approach can process parallelly nominal and feedback robot control.

Another feedforward control algorithm which is based on neural networks is presented by Katic and Vukobratovic [35]. This algorithm is for contact tasks. Connectionist structures are used in non learning control laws. The proposed control law achieves stability and good tracking performance of position and force. Four layer perception network is used as a part as hybrid learning control algorithm. In order to minimize training time and effort, available sensor information is used in the task. The resulting four layer feedforward neural network is used to control both force and position. The problem of tracking a reference trajectory with a constant force reference is solved.

The use of an adaptive feedforward neural network control is for the disturbance rejection problem of a missile seeker is proposed in [36] by Lin and Hsiao. To improve the seeker tracking accuracy, feedforward control is added (Figure 2.3.1). Feedforward controller is realized by a multilayer neural network. The controller can eliminate highly nonlinear disturbance torques. Connecting link masses between neural network layers are updated adaptively to achieve a reasonable performance. Results are compared with controllers without disturbance compensation and it is validated that the disturbance compensation is beneficial for tracking accuracy.

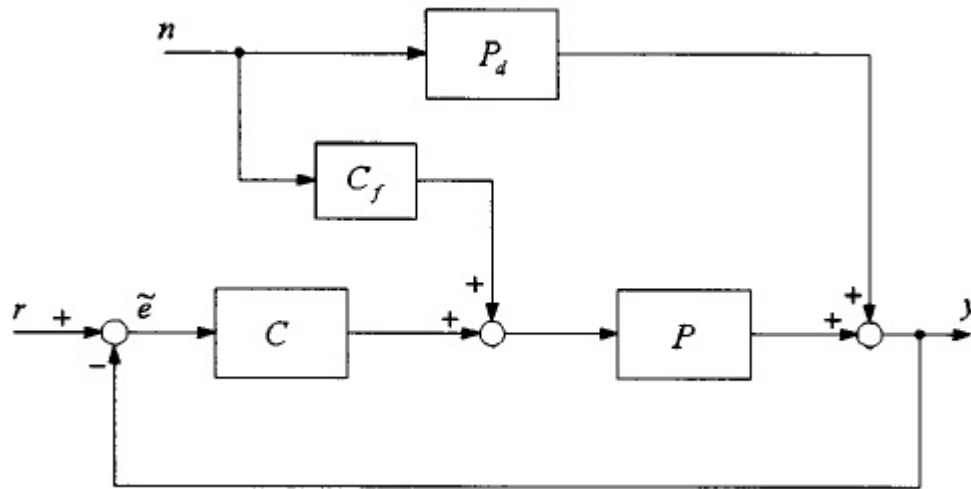


Figure 2.3.1: Feedback-feedforward control system [36]

Feedforward control can be used for flexible joints and flexible links of manipulators. A study by Lanari and Wen on flexible robots proposes a controller structure mainly consisting of a stabilizing feedback loop and a model based feedforward control block. The feedforward control law is applied for flexible joint robots and single link flexible links [37].

In many cases, adaptive feedforward controllers are used for canceling disturbance effects. In the study by Flores, Tang and Osorio [38], a design procedure based on adaptive feedforward control and adaptive feedforward disturbance cancellation is discussed. This controller is implemented by using frequency domain techniques. Resulting model only needs general knowledge of the plant structure. A reduced-order parametric model is used in order to achieve simplified analysis.

In [39], the selection of proportional and derivative gains with computed feedforward control (Figure 2.3.2) of robot manipulators is carried out by using a design procedure. The procedure employs robot dynamics and desired trajectory of the end effector and assures that the closed loop system is locally exponentially stable and has a unique equilibrium point. Here,  $q$  and  $\dot{q}$  are actual position and actual velocity of the robot.  $q_d$ ,  $\dot{q}_d$  and  $\ddot{q}_d$  are desired trajectory, desired velocity and desired acceleration, respectively.  $M(q_d)$  denotes the manipulator inertia matrix,  $C(q_d, \dot{q}_d)$  is the vector of centripetal and corolis torques,  $g(q_d)$  is the vector of gravitational torques.  $K_v$  and  $K_p$  are derivative and proportional gain matrices, respectively.

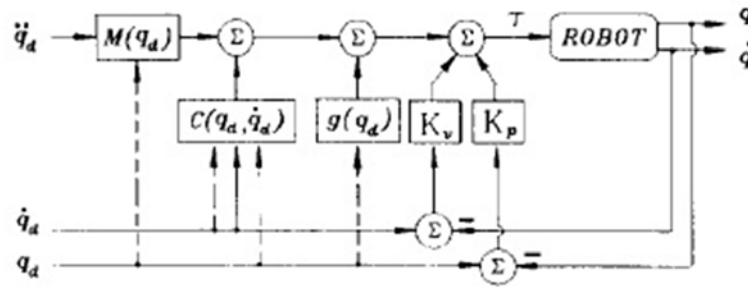


Figure 2.3.2: PD control with computed feedforward [39]

A controller design applicable to both linear and nonlinear models is presented by Zaher *et al.* [40]. The design technique is a combination of Lyapunow based techniques and state feedback. The main goal is to find the best parameter update law that guarantees satisfactory transient performance and stability. Trade off situations between the two concepts are studied. Simulations are carried out on a single-dof robotic arm model In Figure 2.3.3,  $L$  is the arm length,  $m$  represents the arm mass,  $g$  denotes gravity,  $\theta$  is displacement angle and  $u$  represents the actuation input. This study is different from adaptive techniques which estimate unknown parameters by iterative methods. Dynamic parameter estimation is used to predict unknown parameters, and the adaptive feedforward control is used to eliminate the uncertainty of unknown parameters.

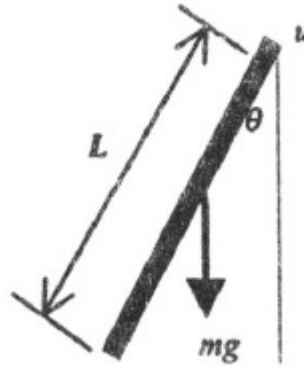


Figure 2.3.3: Single dof robot arm model [40]

Robots with elastic joints have the problem that the product of the angle rotors and the reduction gear ratio does not always correspond to the the link angle. To solve this problem, a multirate feedforward control scheme is proposed in [41] by Shimada and Takeda. State references for elastic joint manipulators are designed. A prototype robot manipulator (Figure 2.3.4) with high precision rotary encoders installed on the output side of the elastic joints is used in the experiments. Experimental results indicate good tracking performance.

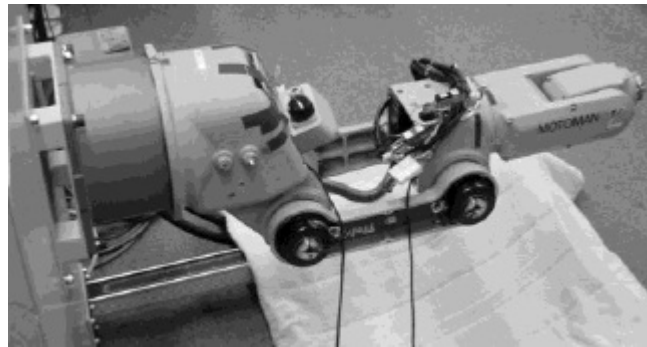


Figure 2.3.4: Prototype robot manipulator [41]

As a robust control method, a variable structure system with a feedforward compensator is proposed in [42] by Duan *et al.* for payload uncertainties for robotic manipulators. Improved tracking precision is achieved by implementing the feedforward compensation. A proportional and integral regulator with feed sequence compensator is used for improving the dynamical performance and lessening the chattering problem. The compensator is asymptotically stable and the tracking performance is found to be satisfactory.

## Chapter 3

### 3. PLANT, FORCE CONTROL AND CONTOUR TRACKING

#### 3.1. The Plant

The manipulator used in this thesis, is SCARA type direct drive two-degrees-of-freedom robot. The manipulator was built in Sabanci University in 2005. The control algorithm of the manipulator runs on a Dspace 1102 DSP based hardware. The board is programmable in C language and therefore new servo routines can be implemented. Base and elbow motors are Yokogawa Dynaserv direct drive motors. These motors are capable of providing position signals with a resolution of 102000 pulses/rev. Elbow motor torque capacity is 40 Nm and the base torque capacity is 200 Nm.

The robot's dynamic equation can be given as

$$\left( \begin{bmatrix} J_1 & 0 \\ 0 & J_2 \end{bmatrix} + D(q_1, q_2) \right) \begin{bmatrix} \ddot{q}_1 \\ \ddot{q}_2 \end{bmatrix} + \left( C(q_1, q_2, \dot{q}_1, \dot{q}_2) + \begin{bmatrix} B_1 & 0 \\ 0 & B_2 \end{bmatrix} \right) \begin{bmatrix} \dot{q}_1 \\ \dot{q}_2 \end{bmatrix} + \begin{bmatrix} F_{c1} \\ F_{c2} \end{bmatrix} + J_M^T \begin{bmatrix} F_{e_x} \\ F_{e_y} \end{bmatrix} = \begin{bmatrix} \tau_1 \\ \tau_2 \end{bmatrix} = \tau \quad (3.1.1)$$

In equation 3.1.1,  $J_1$  and  $J_2$  stand for the rotor inertia parameters of base and elbow, respectively. Their values are taken from manufacturer's documentation. Above,  $D$  is manipulator inertia matrix.  $q_1$  and  $q_2$  are joint angular positions for base joint and elbow joints, respectively.  $\dot{q}_1$  and  $\dot{q}_2$  are first order derivatives of joint angular positions,  $\ddot{q}_1$  and  $\ddot{q}_2$  are angular accelerations.  $C$  is a matrix which is representing centripetal and Coriolis effects.  $B_1$  and  $B_2$  are constant viscous friction coefficients for base and elbow joints, respectively. Viscosity coefficients are obtained experimentally by using force sensors.  $F_{c1}$  and  $F_{c2}$  represent Coulomb friction torques.  $J_M$  is jacobian of the manipulator.

$F_{e_x}$  stands for the force on tool tip in x direction which is applied on the environment, and  $F_{e_y}$  force component of the tool tip in y direction. Lastly,  $\tau_1$  and  $\tau_2$  are the joint actuation torques, which are used to control robot. The SCARA-type manipulator has horizontal kinematic arrangement so gravity effect cannot be seen at the joint dynamics.

The matrix  $D$  can be expressed as:

$$D(q_1, q_2) = \begin{bmatrix} m_1 l_{c1}^2 + m_2 (l_1^2 + l_{c2}^2 + 2l_1 l_{c2} \cos q_2) + I_1 + I_2 & m_2 (l_{c2}^2 + l_1 l_{c2} \cos q_2) + I_2 \\ m_2 (l_{c2}^2 + l_1 l_{c2} \cos q_2) + I_2 & m_2 l_{c2}^2 + I_2 \end{bmatrix} \quad (3.1.2)$$

In 3.1.2,  $m_1$  and  $m_2$  are link masses,  $l_1$  and  $l_2$  are link lengths.  $l_{c1}$  and  $l_{c2}$  are distances of joint center of masses.  $I_1$  and  $I_2$  are link inertias, and  $c_1$  and  $c_2$  are center of mass points. Corresponding values to above constants are given in Table 3.1.1. Center of mass locations and link inertias are computed via CAD models of links (Figure 3.1.1). Center of mass distances and link lengths are shown in Figure 3.1.2.  $I_1$  and  $I_2$  are computed along the principle axes, which are perpendicular to the sketch plane on the center of mass locations. Axes of moment of inertia computation are shown in Figure 3.1.2 too.

$C$  can be expressed as:

$$C(q_1, q_2, \dot{q}_1, \dot{q}_2) = (m_2 l_1 l_{c2} \sin q_2) \begin{bmatrix} -\dot{q}_2 & -(\dot{q}_1 + \dot{q}_2) \\ \dot{q}_1 & 0 \end{bmatrix} \quad (3.1.3)$$

$C$  and  $D$  matrices are calculated by using the Euler-Lagrange method. Numerical values of the matrices and expressions can be found by using parameter values in Table 3.1.1.

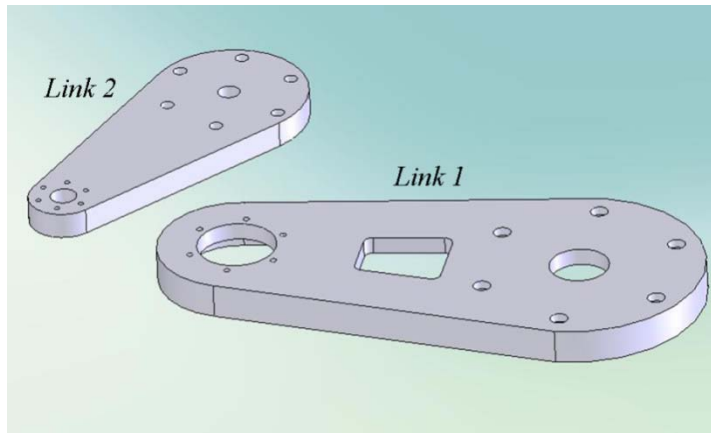


Figure 3.1.1: SCARA type robot arm and link models (picture of assembled links above and CAD drawings of the links below.)

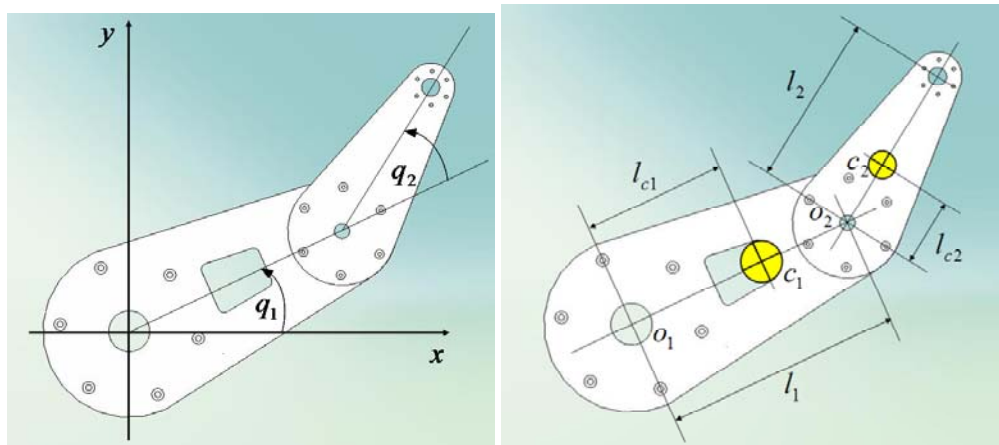


Figure 3.1.2: Robot joint angle descriptions and length parameters (coordinate axes at left, link lengths at right)

Table 3.1.1  
Robot Parameters

Link 1 weight $m_1$ (including elbow motor)	17.9 kg	Link 2 weight $m_2$	3.25 kg
Link 1 inertia $I_1$ (Including elbow motor)	0.54 kg m <sup>2</sup>	Link 2 inertia $I_2$	0.04 kg m <sup>2</sup>
Motor 1 rotor inertia $J_1$	0.167 kg m <sup>2</sup>	Motor 2 rotor inertia $J_2$	0.019 kg m <sup>2</sup>
Link 1 length $l_1$ (Joint center to joint center)	0.4 m	Link 2 length $l_2$ (Joint center to tool center)	0.28 m
Link 1 joint to center of mass distance $l_{c1}$	0.277 m	Link 2 joint to center of mass distance $l_{c2}$	0.09 m
Joint 1 viscous friction coefficient $\hat{B}_1$	3 Nms/rad	Joint 2 viscous friction coefficient $\hat{B}_2$	0.6 Nms/rad

### 3.2. Force control and the contour tracking algorithm

As mentioned before manipulator dynamic equation is

$$\cdot \left( \begin{bmatrix} J_1 & 0 \\ 0 & J_2 \end{bmatrix} + D \right) \begin{bmatrix} \ddot{q}_1 \\ \ddot{q}_2 \end{bmatrix} + \left( C + \begin{bmatrix} B_1 & 0 \\ 0 & B_2 \end{bmatrix} \right) \begin{bmatrix} \dot{q}_1 \\ \dot{q}_2 \end{bmatrix} + \begin{bmatrix} F_{c1} \\ F_{c2} \end{bmatrix} + J_M^T \begin{bmatrix} F_{e_x} \\ F_{e_y} \end{bmatrix} = \begin{bmatrix} \tau_1 \\ \tau_2 \end{bmatrix} = \tau. \quad (3.2.1)$$

Since due to the nature of contour tracking tasks velocity and acceleration is very low, effects of inertial and corrolis terms can be neglected. A simplified version of the dynamic equation of the manipulator can hence be expressed as

$$\begin{bmatrix} F_{c1} \\ F_{c2} \end{bmatrix} + J_M^T \begin{bmatrix} F_{e_x} \\ F_{e_y} \end{bmatrix} = \begin{bmatrix} \tau_1 \\ \tau_2 \end{bmatrix} = \tau. \quad (3.2.2)$$

Based on the equation above, the following contour tracking control law is proposed in [43] by Jatta *et al.*:

$$\tau = J_M^T (U_{PID} + K_R R), \quad (3.2.3)$$

$$U_{PID} = \begin{bmatrix} U_{PID_V} \\ U_{PID_F} \end{bmatrix}, \quad (3.2.4)$$

$$K_R = \begin{bmatrix} k_V & 0 \\ 0 & k_F \end{bmatrix} \quad (3.2.5)$$

$$R = \begin{bmatrix} ref_t \\ ref_n \end{bmatrix}. \quad (3.2.6)$$

Here,  $U_{PID_V}$  is PID action for tangential velocity control.  $U_{PID_F}$  is PID action for normal force control.  $k_V$  and  $k_F$  are feedforward gains of tangential velocity and normal force.  $ref_t$  and  $ref_n$  are reference tangential velocity and reference normal force, respectively.

This thesis adopts the method in [43] partially. Although the main control law used in the thesis is the same as in (3.2.3) the way of computation of  $K_R$  and the reference signal are different. A fuzzy parameter adjustment system is used for the online determination of  $K_R$ , as is discussed in the next chapter. This chapter considers the control algorithm without fuzzy online tuning and presents simulation results with manual tuning of this matrix along with other controller parameters.

The control parameters  $k_V$  and  $k_F$  tuned in by trial and error manually, after tests and trials the values that gave more successful results are chosen as final values. They are listed below (Table 3.2.1).

Table 3.2.1  
Controller Parameters

$k_V$	1.5
$k_F$	1.5

PID control is a well known mathematical algorithm used to eliminate the error between the desired reference state and the actual state of the system. The error is the

difference between the data obtained by sensors, which are embedded in the system, and the reference signal which is implemented within the control software. The expression for error in this case are

$$e_V = ref_t - J_M \dot{q}, \quad (3.2.7)$$

$$e_F = ref_n - F_{e_x}, \quad (3.2.8)$$

$$E(t) = \begin{bmatrix} e_V \\ e_F \end{bmatrix}. \quad (3.2.9)$$

$U_{PID}$  is computed as

$$U_{PID} = K_P E(t) + K_I \int E(t) + K_D E'(t), \quad (3.2.10)$$

where the coefficient matrices are explicitly written as

$$K_P = \begin{bmatrix} k_{P_f} & 0 \\ 0 & k_{P_v} \end{bmatrix} \quad (3.2.11)$$

$$K_I = \begin{bmatrix} k_{I_f} & 0 \\ 0 & k_{I_v} \end{bmatrix} \quad (3.2.12)$$

$$K_D = \begin{bmatrix} k_{D_f} & 0 \\ 0 & k_{D_v} \end{bmatrix} \quad (3.2.13)$$

Force and velocity control parameters,  $k_{P_f}$ ,  $k_{P_v}$ ,  $k_{I_f}$ ,  $k_{I_v}$ ,  $k_{D_f}$  and  $k_{D_v}$  are tuned by trial and error too. Final values are chosen as they have best results when compared to other trial values. Their values are listed in Table 3.2.2.

Table 3.2.2  
Force, velocity control parameters

$k_{P_f}$	2
$k_{I_f}$	0
$k_{D_f}$	0.1
$k_{P_v}$	1000
$k_{I_v}$	100
$k_{D_v}$	3

The full robot model (3.1.1) and the controller structure explained above are used in the simulations to track the surface of a wall. The wall surface is represented with a line equation as follows:

$$y_{wall} = b_{wall} (x_{wall} - c_{wall}) / a_{wall} + d_{wall} . \quad (3.2.14)$$

$y_{wall}$  and  $x_{wall}$  are wall's Cartesian coordinates of a generic point on the the wall,  $a_{wall}$ ,  $b_{wall}$ ,  $c_{wall}$  and  $d_{wall}$  are wall position and orientation parameters and their values are presented in Table 3.2.3. The tool contact with wall is modeled as a spring and damper system. Normal force  $F_N$  on its surface is computed with equation

$$F_N = F_k + F_b . \quad (3.2.15)$$

Here,  $F_k$  is wall spring force,  $F_b$  is wall damper force. Spring force is nonzero when the simulated tool tip of the manipulator penetrates the wall surface. With the specific choices of the wall position and orientation parameters in Table 3.2.2, the wall is parallel to the y-axis and the penetration occurs when the tool tip x position is larger than the wall position along the x-axis. Damper force nonzero when the x-directional velocity of the end effector is positive while in contact.

$$F_k = k_{wall} (x_e - x_{wall}) , \quad (3.2.16)$$

$$F_b = k_{b-wall} V_{e_x}, \quad (3.2.17)$$

$$J_M \begin{bmatrix} q_1 \\ q_2 \end{bmatrix} = \begin{bmatrix} x_e \\ y_e \end{bmatrix}, \quad (3.2.18)$$

$$J_M \begin{bmatrix} \dot{q}_1 \\ \dot{q}_2 \end{bmatrix} = \begin{bmatrix} V_{e_x} \\ V_{e_y} \end{bmatrix}. \quad (3.2.19)$$

Here,  $k_{wall}$  is walls spring constant,  $k_{b-wall}$  is walls damper constant, and  $x_e$  and  $y_e$  are end effector's position in Cartesian coordinates.  $V_{e_x}$  and  $V_{e_y}$  are end effector's velocity components in Cartesian representation. Wall contact model parameters are shown in Table 3.2.3.

Table 3.2.3  
Wall parameters

$k_{wall}$	100000
$k_{b-wall}$	200
$a_{wall}$	0
$b_{wall}$	-2
$c_{wall}$	0.5
$d_{wall}$	0.5

Figure 3.2.1 shows the wall and end effector position obtained in a simulation scenario. In this scenario, the tool tip is initially positioned at a distance from the wall. An x-directional (normal) force reference of 10 Newtons and a y-directional (tangent) position reference are applied simultaneously with the control law in (3.2.3). The y-directional position reference corresponds to a trapezoidal velocity curve with a 1 cm per second speed and 1 s acceleration/deceleration time. A distance on 5 cm is to be travelled in the positive y-direction on the wall surface. As can be observed form the figure, firstly, the end effector reaches and hits the wall. This is followed by a phase in which the tool tip tries to track the

wall. However, the tool cannot track the position reference. The distance between end effector and contact surface is not constant.

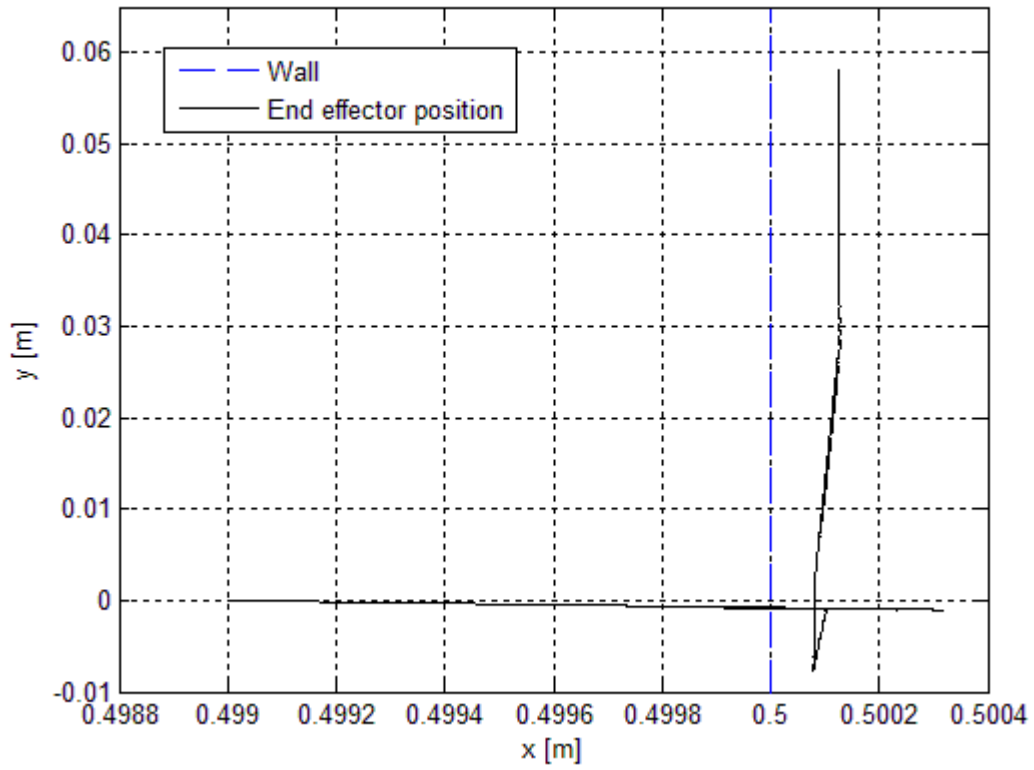


Figure 3.2.1: Wall and end effector positions

Figure 3.2.2 depicts the reference and the actual normal force curves. Although the reference force signal is 10 Nm the actual normal force varies between 7.8 Nm and 12.9 Nm.

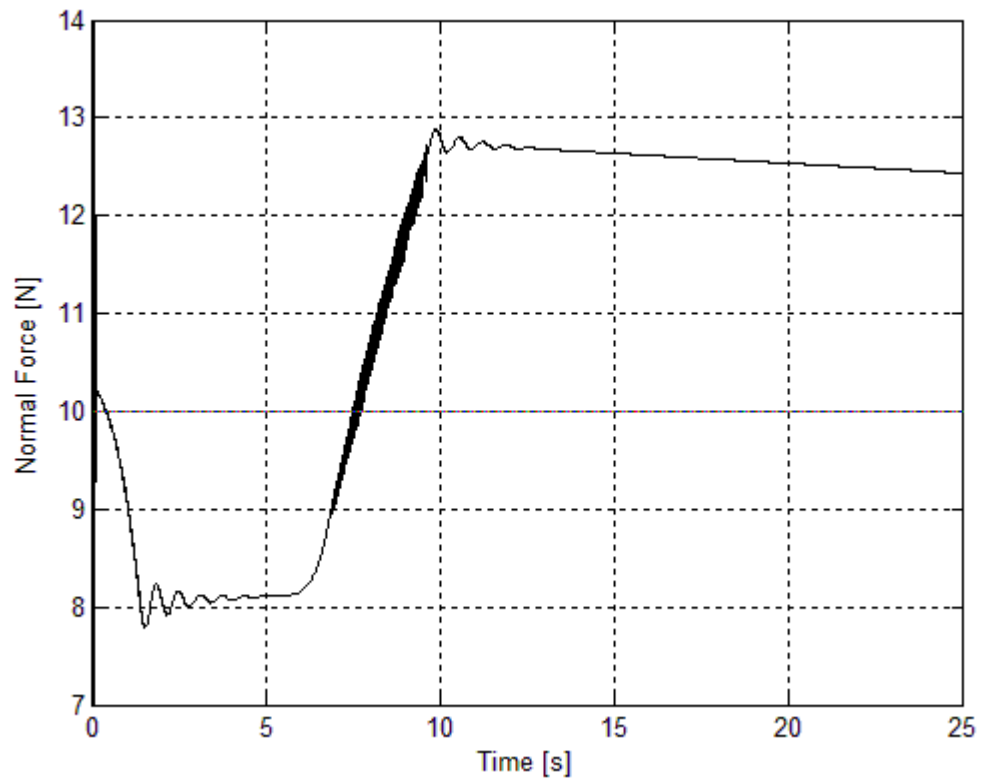


Figure 3.2.2: Actual and reference normal force: actual concrete, reference dashed line

Next, Figure 3.2.3 shows actual y-position of the end effector together with the y-directional position reference. Reference signal cannot be tracked and error varies between -0.01 and 0.01 meters.

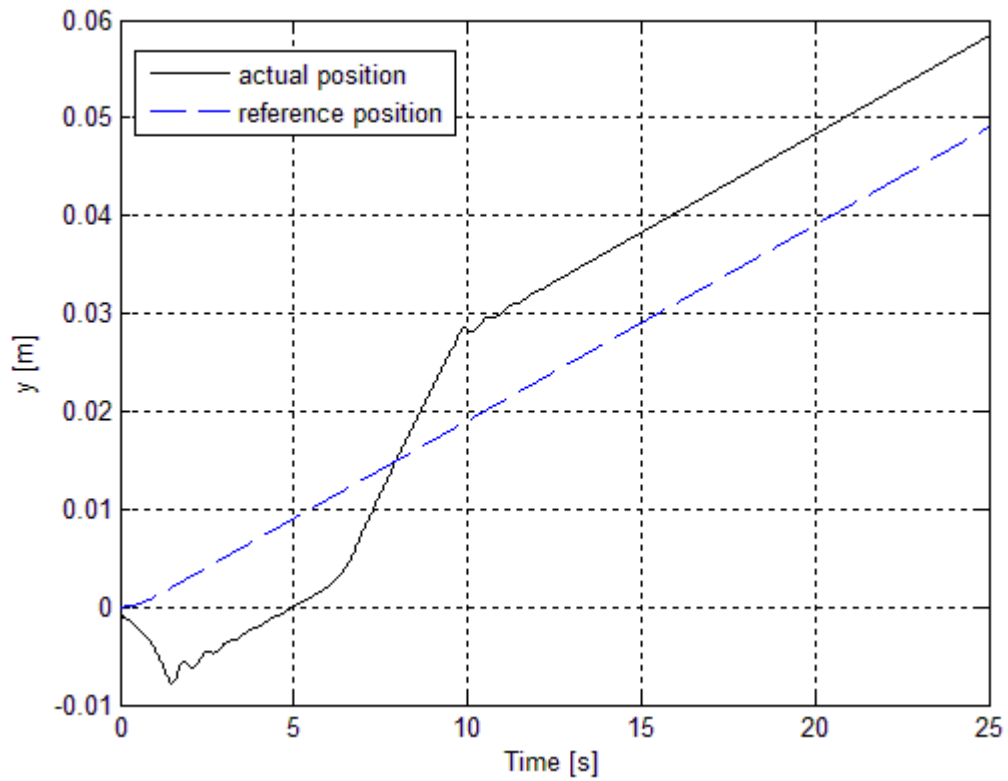


Figure 3.2.3: Actual and reference y-axis position; actual concrete and reference dashed line.

Figure 3.2.4 shows elbow and shoulder joint positions. Steady state cannot be reached; positions of shoulder and elbow are varying.

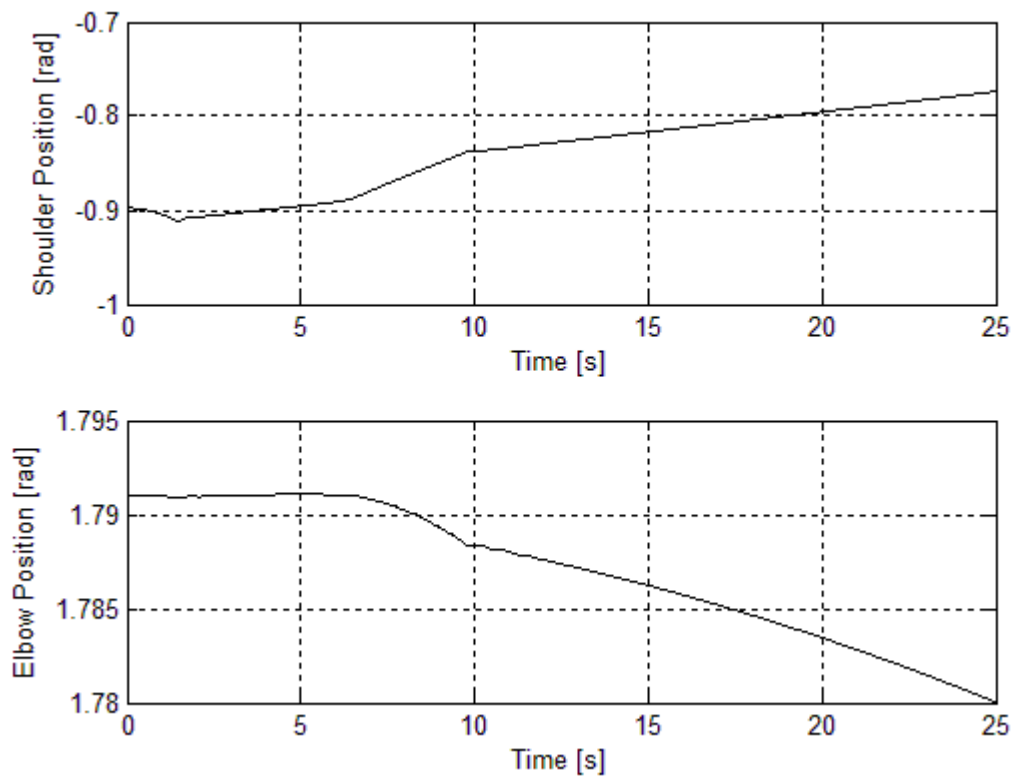


Figure 3.2.4: Time dependent shoulder and elbow positions.

Finally, Figure 3.2.5 presents the corresponding shoulder and elbow joint torques. The control torques are smooth, however they do not exhibit dynamic control effort to overcome tracking errors.

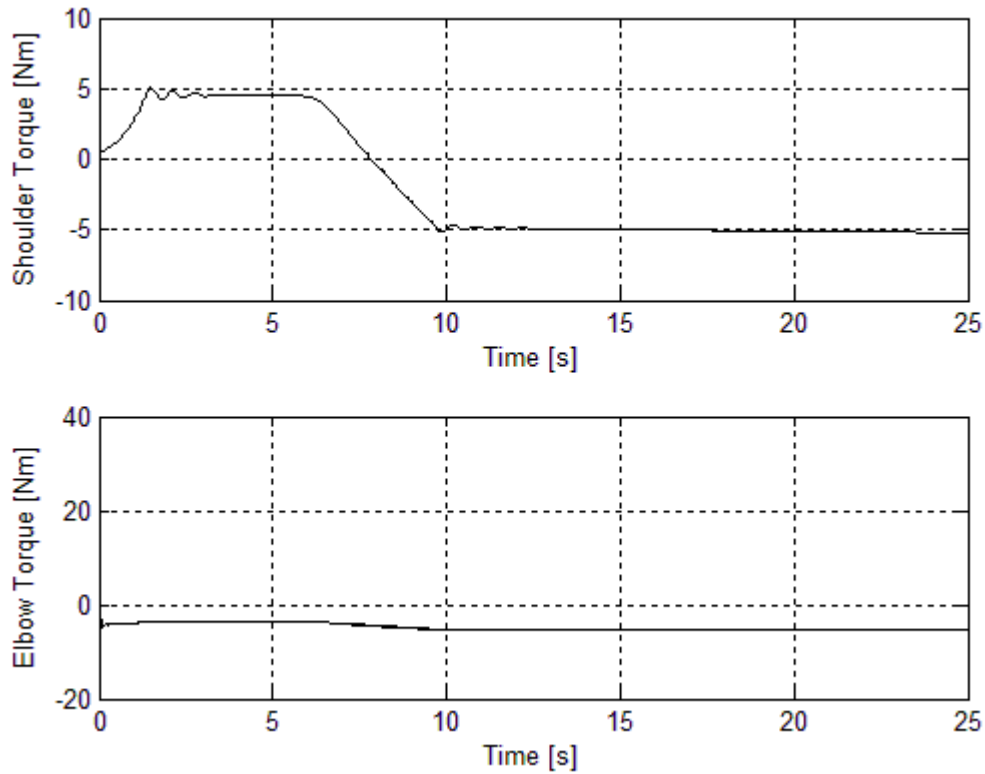


Figure 3.2.5: Time dependent shoulder and elbow torques.

The results presented with the manually tuned control method are far from being satisfactory. To that end, further improvements are necessary. The next chapter approaches this problem with an online fuzzy parameter adjustment technique.

In this chapter:

- The model of the 2-DOF SCARA type manipulator is built.
- The wall model as a contact surface for contour tracking algorithm is proposed.
- PID control parameters tuned by trial and error method and PID controller is added to model.

- Feedforward control with constant feedforward parameters is added to the controller, feedforward parameters are tuned by trial and error, manually.
- Resulting plant and controller system is simulated and results are explained.

## Chapter 4

### 4. FUZZY PARAMETER ADJUSTMENT

As mentioned above, the results with the manually tuned contour tracking algorithm are not satisfactory. Simulations in previous chapter are carried out with parameters that are tuned by trial and error. A fuzzy parameter adjustment approach is proposed in this chapter to tune the feedforward gains  $k_V$  and  $k_F$  of the system. This is an online tuning system. The developed fuzzy system aims to find a balance between chattering in control signal  $U_{PID}$  and tangential velocity and normal force errors.

Chattering can be defined as high frequency oscillations in a control signal. It is an indicator of control effort. However, too much chattering can invoke high frequency manipulator dynamics. It is also undesirable for mechanical parts like bearings and transmission elements. In order to assess the amount of chattering in the control signals a chattering variable,  $\Gamma$ , is introduced in this thesis as

$$\Gamma_k = \begin{bmatrix} \Gamma_{1k} \\ \Gamma_{2k} \end{bmatrix} = \Gamma_{k-1} + \text{abs} \left( \begin{bmatrix} U_{PID_{F_k}} \\ U_{PID_{V_k}} \end{bmatrix} - \begin{bmatrix} U_{PID_{F_{k-1}}} \\ U_{PID_{V_{k-1}}} \end{bmatrix} \right), \quad (4.1)$$

where  $k$  stands for the discrete time index.

The main idea after the fuzzy parameter adjustment method proposed is:

- (i) When chattering is small, control parameter is smooth and the controller activity is low. In order to increase the control activity control parameter (feedforward gain) should be increased.
- (ii) When chattering is large, it means that controller activity is high. This may harm the robotic mechanical hardware. Therefore, the control parameter should be decreased.

This logic alone can be applied to adjust feedforward control parameters; however, this information does not contain data about the end effector is in contact with the surface. Therefore another variable should be used in addition to chattering variable. Normal force and tangential velocity errors become useful at this point. A similar approach is used for these errors:

- (i) When errors are low, control parameters are suitable; therefore do not adjust feedforward control parameter.
- (ii) When errors are high, control parameters are not sufficient; therefore increase (or decrease) control parameter.

Combining the four principles above, a fuzzy rule table is created (Table 4.1) for the magnitude of the required change in the feedforward gains every sampling instant (2 ms in the simulations presented in this thesis). The table is applied for the feedforward gains responsible with the feedforward control actions in the tangential and normal directions independently. The fuzzy rules only decide upon the required magnitude of the change on the gain. The sign of the change is determined by the sign of the corresponding error (tangential position error or normal force error). The numerical values for the rule strengths  $\Delta K_{RSS}$ ,  $\Delta K_{RSB}$ ,  $\Delta K_{RBS}$  and  $\Delta K_{RBB}$  are listed in Table 4.2.

Table 4.1  
Fuzzy rule parameters

		$\Gamma$	
		Small $\Gamma$	Big $\Gamma$
$E$	Small $E$	$\Delta K_{RSS}$ <i>Rule A</i>	$\Delta K_{RSB}$ <i>Rule B</i>
	Big $E$	$\Delta K_{RBS}$ <i>Rule C</i>	$\Delta K_{RBB}$ <i>Rule D</i>

Table 4.2  
Fuzzy rule values

$\Delta K_{RSS}$	1
$\Delta K_{RSB}$	0
$\Delta K_{RBS}$	10
$\Delta K_{RBB}$	3

Feedforward control gains are updated with the equation:

$$K(k) = K(k-1) + \lambda \Delta K(k-1) \text{sgn}(e). \quad (4.2)$$

Here,  $K$  signifies  $k_v$  or  $k_F$  and  $e$  stand for the tangential position error or the normal direction force error.  $\text{sgn}$  is the sign function. The same formula is used for the parameter update of the two directional feedforward gains. The fuzzy rules, when used for the adjustment of  $k_F$  use  $\Gamma_1$  and the force error as the input variables. When used for  $k_v$  the chattering input is  $\Gamma_2$  and the error input is the y-directional position error. It should also be mentioned that the error signal absolute values are used as the inputs to the fuzzy system. Therefore, it is the sign function in (4.2) what makes the feedforward gains increase or decrease.  $\lambda$  is a small gain (0.0001 in the simulations) which is used for smooth variation of the feedforward gain parameters.  $k$  is the time index variable.

The change magnitude  $\Delta K$  in feedforward gain in (4.2) can be expressed as

$$\Delta K = \frac{\mu_{SmallE}(E)\mu_{Small\Gamma}(\Gamma)\Delta K_{RSS} + \mu_{BigE}(E)\mu_{Small\Gamma}(\Gamma)\Delta K_{RBS} + \mu_{BigE}(E)\mu_{Big\Gamma}(\Gamma)\Delta K_{RBB}}{\mu_{SmallE}(E)\mu_{Small\Gamma}(\Gamma) + \mu_{BigE}(E)\mu_{Small\Gamma}(\Gamma) + \mu_{SmallE}(E)\mu_{Big\Gamma}(\Gamma) + \mu_{BigE}(E)\mu_{Big\Gamma}(\Gamma)}. \quad (4.3)$$

Here,  $\mu_{SmallE}$ ,  $\mu_{BigE}$ ,  $\mu_{Small\Gamma}$  and  $\mu_{Big\Gamma}$  are trapezoid membership functions. They are shown in Figure 4.1 and Figure 4.2.  $\Gamma_{Small}$ ,  $\Gamma_{Big}$ ,  $E_{Small}$  and  $E_{Big}$  are the corner values of trapezoid functions. They are also chosen by trial and error method manually. Their numerical values are listed in Table 4.3.

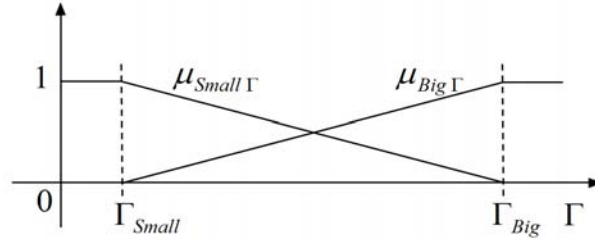


Figure 4.1: Trapezoid functions for  $\Gamma$

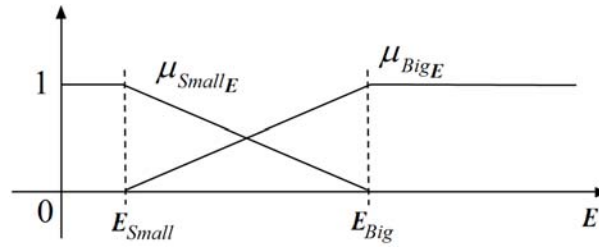


Figure 4.2: Trapezoid functions for  $E$

Table 4.3  
Corner values

$\Gamma_{Small}$	3
$\Gamma_{Big}$	200
$E_{Small}$	0.1
$E_{Big}$	1

It can be noted that the choice of membership functions and rule base parameters satisfies the previously mentioned chattering and error principles. Rules A to D in Table 4.1 are explained below in detail.

Rule A is used if the chattering and the error both are small. In that case feedforward control gain  $K$  is increased (or decreased if the error is negative) by the rate  $\Delta K_{RSS}$ . Since error is low, drastic changes in feedforward gain is unnecessary, but small chattering shows that control action can be changed safely, therefore gain should increased (or decreased if the error is negative) with a relatively little rate.

Rule B is applied when the error is small but chattering is big. Rule B's rate is  $\Delta K_{RSB}$  which is set to zero. It means that when this condition is valid feedforward control gain is kept unchanged. Small error and big chattering is a desired scenario, assuming that

chattering increased to this level gradually. Control effort is high and error is low. So this region chosen as a dead zone and tuning action in this region is kept inactive. The feedforward action should not get bigger in order not to increase chattering further, and it should not be decreased, because this could cause the error to grow.

Rule C is invoked when the chattering is small while the error is high. This region represents the worse condition since we desire a certain chattering level and low error. This regions' change rate is  $\Delta K_{RBS}$ . This constant represents the biggest rate in Table 4.1. The feedforward gain is increased (or decreased if the error is negative) rapidly should this situation arise.

Rule D is for the case when both the chattering and the error are high. For this situation, error should be decreased; therefore a modification in feedforward control gain is necessary. The change rate  $\Delta K_{RBB}$  chosen bigger than rule A's change rate and smaller than rule C's rate. Feedforward control gain is increased (or decreased if the error is negative) for this region too.

In following parts of this section, simulation results of this fuzzy parameter adjustment system are presented. In the simulations in the previous chapter, feedforward gain is tuned by hand; however, for the following simulations, the fuzzy tuning system is used to tune feedforward control gain online. The fuzzy system variables and parameters are newly introduced as tabulated, while other control and plant parameters and references are preserved as used in the previous simulation.

In Figure 4.3 wall and end effector positions are shown. There are no noticeable changes between the previous simulation and current simulation as observed in this figure. This is because temporal information and contact force data is missing in this x-y trajectory plot.

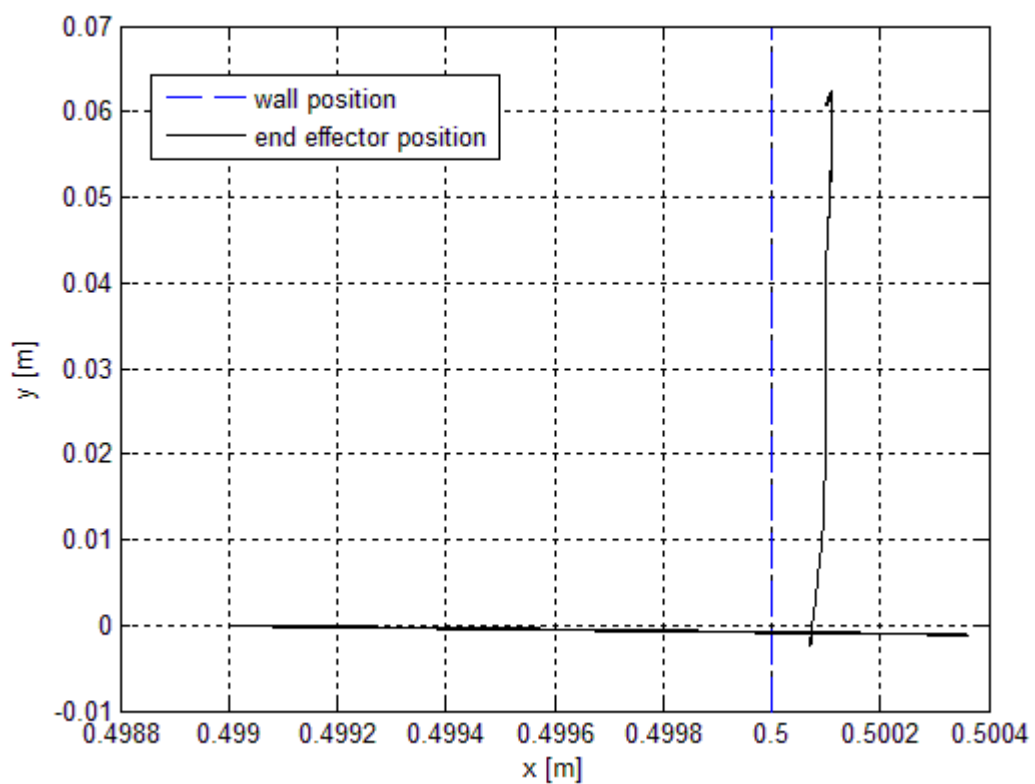


Figure 4.3: Wall and end effector positions

Figure 4.4 shows position and normal force errors. In normal force error significant improvement is visible. The force reference of 10 N is achieved to a large extent. The y-directional position tracking is improved too. Position tracking error goes to steady state after 8 seconds.

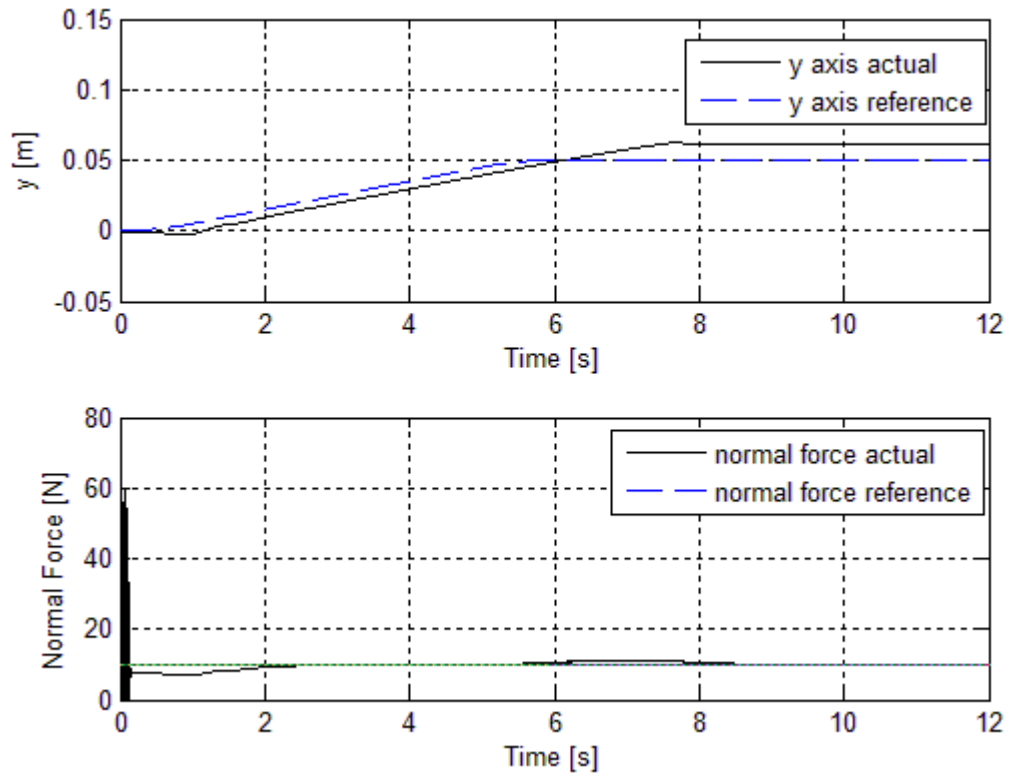


Figure 4.4: Actual and reference y-axis positions (top); actual and reference normal force (bottom).

Figure 4.5 shows shoulder and elbow joint positions. Elbow position chattering occurs when end effector touches wall at first time. However chattering dies before 0.5 seconds rest of the signal is smooth.

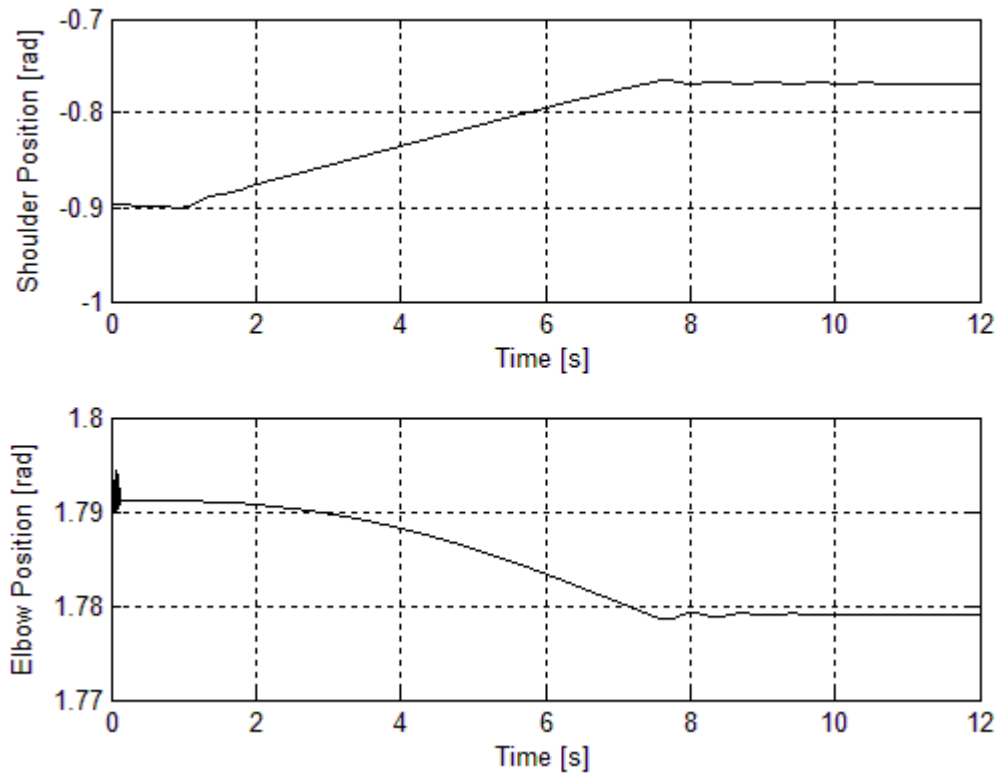


Figure 4.5: Shoulder and elbow positions in polar coordinates

Next two figures, i.e. Figure 4.6 and Figure 4.7, show chattering variable values for elbow and shoulder joints together with corresponding control torque curves. Although the chattering computations carried out used the orthogonal control actions  $U_{PID_F}$  and  $U_{PID_V}$  as inputs, the chattering on the joint control torques are significant too. These control torques should not exhibit high levels of oscillatory behavior for the sake of mechanical parts. The chattering curves in Figure 4.6 and Figure 4.7 are found by applying (4.1) directly on the control torques. The figures show that the chattering in the control torques remains quite low, except for a short while in the phase of touching the wall.

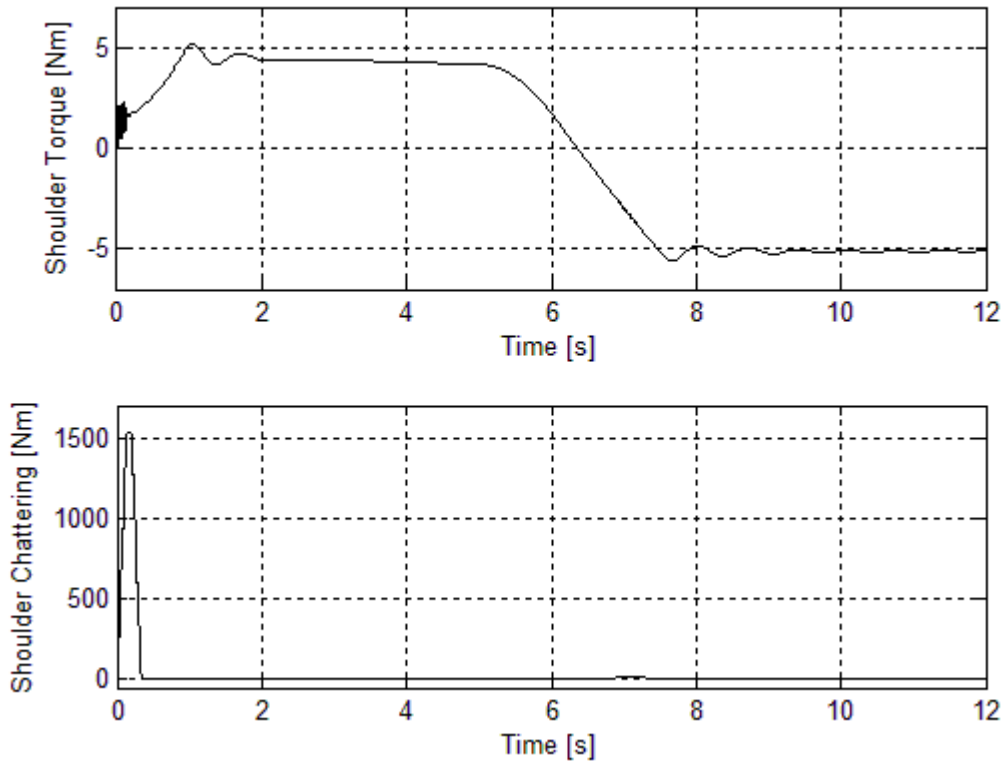


Figure 4.6: Shoulder torque (top) and chattering (bottom).

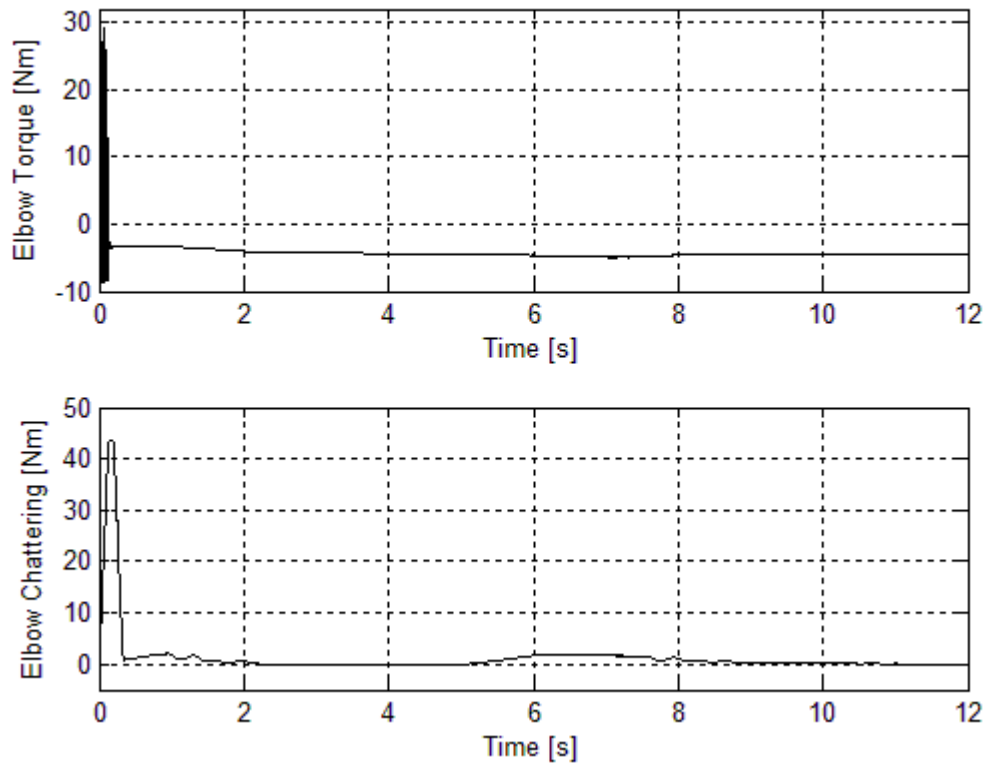


Figure 4.7: Elbow torque (top) and chattering (bottom).

The evolution of the feedforward gain parameters  $k_F$  and  $k_V$  is shown in Figure 4.8. The initial value of both parameters is 1. The fuzzy tuning method tunes them so that the applied feedforward control matched the demands of the situation.

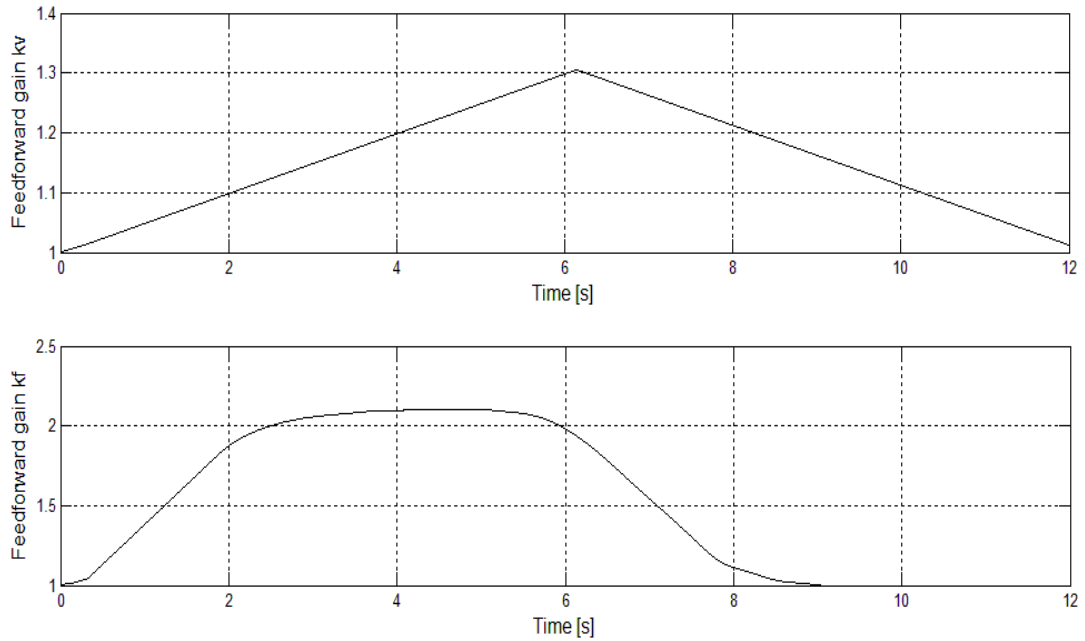


Figure 4.8: Feedforward gain parameters

Figures 4.9 and Figure 4.10 compare the control results with and without the fuzzy tuning on the same graph. It is observed that with fuzzy parameter tuning, the resultant adjustment leads to more successful results. Normal force error in this case is significantly smaller. Furthermore, the tangential error converges to a constant value with fuzzy adjustment while with the constant-parameter feedforward control, normal error and tangential error cannot be stabilized. As we can see in these figures, the system with fuzzy adaptation moves to a steady state in both normal force and tangential directions more rapidly.

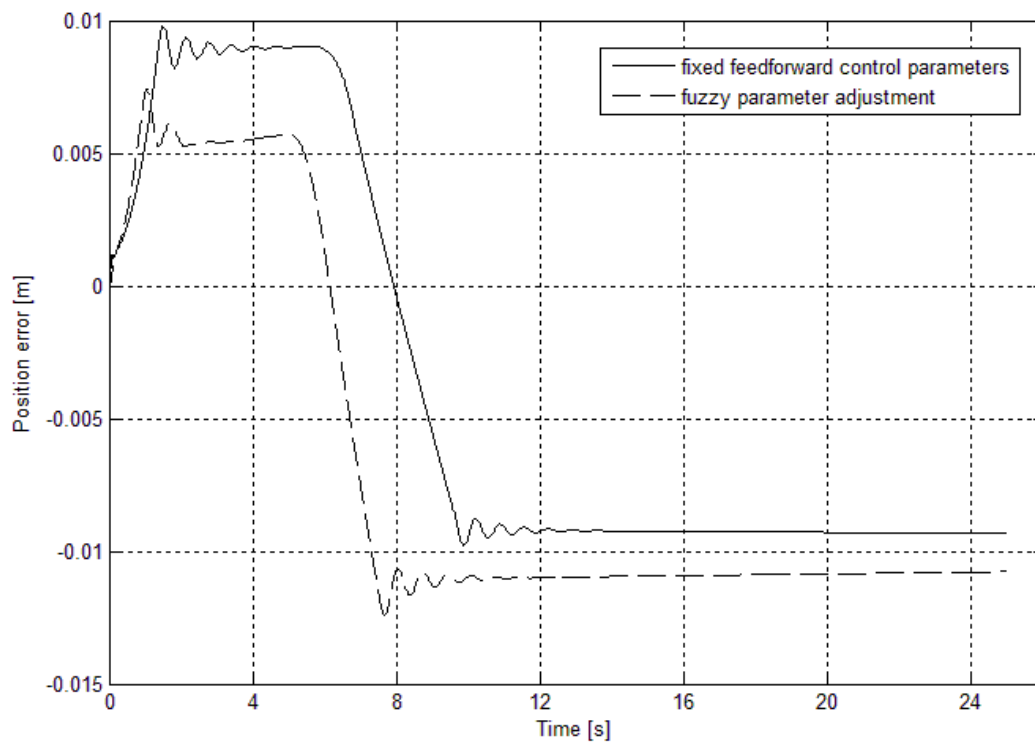


Figure 4.9: Error of y-axis positions for two simulations

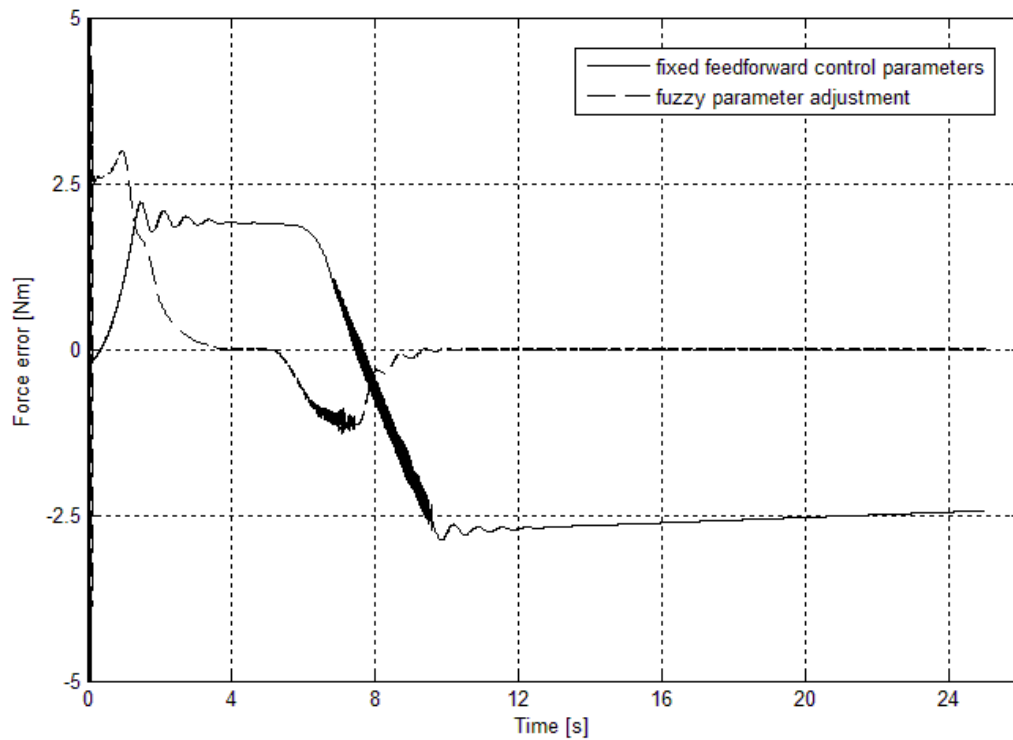


Figure 4.10: Error of normal force for two simulations

In this chapter:

- A chattering variable is introduced.
- A rule bases for fuzzy parameter adjustment is proposed.
- Chattering variable and normal force and tangential errors are used to tune feedforward parameters using fuzzy parameter adjustment.
- The previous controller mentioned at Chapter 3 is improved.
- Simulation results are explained.
- A comparison between the two controllers is presented.
- Improvement in controller performance is achieved.

## Chapter 5

### 5. Conclusion

In this thesis, a contour tracking problem is investigated. A hybrid control method with position control action in the tangential direction and explicit force control in the normal direction is chosen from the literature and is used as a controller backbone. This controller contains building blocks for PID actions and feedforward control. The study in this thesis shows that feedforward control action does not provide satisfactory tracking results when applied with constant gain parameters.

The thesis proposes an online tuning method for these gains. The tuning method relies on fuzzy logic. A control effort indicator termed as a chattering variable is introduced. This chattering variable, together with the tangential position and normal force errors, is used as an input of the fuzzy tuning algorithm.

Simulation results carried out with the model of a direct drive SCARA-type manipulator indicate that the online fuzzy tuning method improves the reference following performance in both the position and force control directions significantly. This makes the proposed method a candidate for implementation on real robots.

Application of this control scheme on a real SCARA-type manipulator considered as a future work.

## References

- [1] Visioli, A., Legnani, G., "On the Trajectory Tracking Control of Industrial SCARA Robot Manipulator," IEEE Transactions on Industrial Electronics, vol. 49, no. 1, pp. 224-232, 2002.
- [2] Hsu, F., Fu, L., "Adaptive Fuzzy Hybrid Force/Position Control for Robot Manipulators Following Contours of an Uncertain Object," Proceedings of the 1996 IEEE International Conference on Robotics and Automation, Minneapolis-Minnesota, pp. 2232-2237, April 1996.
- [3] Muto, S., Shimokura, K., "Teaching and Control of Robot Contour Tracking Using Contact Point Detection," Proceedings of 1994 IEEE International Conference on Robotics and Automation, San Diego-CA, pp. 674-681, May 1994.
- [4] Chen, H., "Automated Industrial Robot Path Planning for Spray Painting Process: A Review," 4<sup>th</sup> IEEE Conference on Automation Science and Engineering, Arlington-VA, pp. 522-527, August 2008.
- [5] Ahmad, S., Lee, C. N., "Shape Recovery from Robot Contour-Tracking with Force Feedback," Proceedings of the 1990 IEEE International Conference on Robotics and Automation, Cincinnati-OH, pp. 447-452, May 1990.
- [6] Chen, Q., Zhu, S., Wang, X., Wu, W., "Analysis on an Uncalibrated Image-Based Visual Servoing for a 6 DOF Industrial Welding Robots," Proceedings of 2012 IEEE Conference on Mechatronics and Automation, Chengdu-China, pp. 2013-2018, August 2012.
- [7] Radi, M., Reinhart, G., "Industrial Haptic Robot Guidance System for Assembly Processes," IEEE International Workshop on Haptic Audio Visual Environments and Games, Lecco-Italy, pp. 69-74, November 2009.
- [8] Skoglund, A., Iliev, B., Kadmiry, B., Palm, R., "Programming by Demonstration of Pick-and-Place Tasks for Industrial Manipulators using Task Primitives," proceedings of the 2007 IEEE International Symposium on Computational Intelligence in Robotics and Automation, Jacksonville-USA, pp. 368-373, June 2007.

- [9] Yu, K., Kieffer, J., "Robotic Force/velocity Control for Following Unknown Contours of Granual Materials," Control Engineering Practice, vol. 7, pp. 1249-1256, 1999.
- [10] Liu, M. H., "Robotic Deburring Based on Fuzzy Force Control," Proceedings of the 1992 IEEE/RSJ International Conference on Intelligent Robots and Systems, Raleigh-NC pp. 782-789, July 1992.
- [11] Palm, R., "Sliding Mode Fuzzy Control," IEEE International Conference on Fuzzy Systems, San Diego-CA, pp. 519-526, March 1992.
- [12] Borgan, S., Kovacic, Z., "Fuzzy Rule-Based Adaptive Force Control of a Single Dof Mechanisms," Proocedings of the 1993 International Symposium on Intelligent Control, Illinois-USA pp. 469-474, August 1993.
- [13] Kiguchi, K., Fukuda, T., "Robot Manipulator Contact Force Control Application of Fuzzy-Neural Network," IEEE International Conference on Robotics and Automation, Nagoya-Japan, pp. 875-880, May 1995.
- [14] Kiguchi, K., Fukuda, T., "Fuzzy Neural Controller for Robot Manipulator Force Control," Yokohama-Japan, pp. 869-874, March 1995.
- [15] Shibata, M., Murakami, T., "A Unified Approach to Position and Force Control by Fuzzy Logic," IEEE Transactions on Industrial Electronics, vol. 43, no. 1, pp. 81-87, 1996.
- [16] Teeter, J., Chow, M. "A Novel Fuzzy Friction Compansation Approach to Improve the Performance of a DC Motor Control System," vol. 43, no. 1, pp. 113-120, 1996.
- [17] Kiguchi, K., Fukuda, T., "Fuzzy Neural Friction Compansation Method for Robot Manipulator During Position/Force Control," Proceedings of the 1996 IEEE International Conference on Robotics and Automation, Minneapolis-Minnesota, pp. 372-377, April 1996.
- [18] Langari, R., Hyun, D., "Fuzzy Logic Based Compansation of Friction in Low Speed Motion Control," Proceedings of the 2011 IEEE International Symposium on Intelligent Control, Mexico City-Mexico, pp. 337-342, September 2001.
- [19] Lin, F., "Robust Fuzzy Neural Network Sliding-Mode Control of Two-Axis Motion Control System," IEEE Transactions on Industrial Electronics, vol. 53, no. 4, pp. 1209-1225, 2006.

- [20] Hung, V., Na, U. J., "Adaptive Neural Fuzzy Control For Robot Manipulator Friction and Disturbance Compensation," International Conference on Control, Automation and Systems, Seoul-Korea, pp. 2569-2574, October 2008.
- [21] Wang, F. Luo, Z., Liu, H., Wang, L., "Impedance Model Based Fuzzy Force Control for Robot Manipulator Contacting with a Constrained Surface with Uncertain Errors," Proceedings of the 2010 IEEE International Conference on Robotics and Biomimetics, Tianjin-China, pp. 1555-1558, December 2010.
- [22] Wang, Y., Wang, D., "Extraction and Adaptation of Fuzzy Rules for Friction Modeling and Control Compensation," IEEE Transactions on Fuzzy Systems, vol. 19, no. 4., pp. 682- 693., 2011.
- [23] Plius, M. P., Yilmaz, M., Seven, U., Erbatur, K., "Fuzzy Controller Scheduling for Robotic Manipulator Force Control," The 12<sup>th</sup> IEEE International Workshop on Advanced Motion Control, Sarajevo-Bosna and Herzegovina, March 2012.
- [24] Junjian, L., Tie, Z., "Fuzzy PD Compliance Control of 6 Degrees-of-Freedom Robot Using Disturbed Force Sense," Proceedings of the 2012 IEEE International Conference on Robotics and Biomimetics, Guangzhou-China, pp. 1674-1679, December 2012.
- [25] Zhen, L., Xu, L., "On-Line Fuzzy Tuning of Indirect Field Oriented Induction Machine Drives," IEEE Transactions on Power Electronics, vol. 13, no. 1, pp. 369-374, 1996.
- [26] Javaheri, H., Vossoughi, G. R., "Sliding Mode Control with Online Fuzzy Tuning: Application to a Robot Manipulator," Proceedings of the IEEE International Conference on Mechatronics & Automation, Niagara Falls-Canada, pp. 1357-1362, July 2005.
- [27] Li, Z., Lang, D., Chen, G., "Fuzzy Self Tuning of Parameters Online for Human Simulated Intelligent Controller," Proceedings of the IEEE International Conference on Systems, Man and Cybernetics, Montreal-Que, pp. 2402-2407, October 2007.
- [28] Truong, D. Q., Ahn, K. K., Yoon, J. I., Jin, M., Choi, C. T., "Design of An Online Tuning Modified-Grey Fuzzy PID Controller for Nonlinear Systems," Proceedings of the 2011 International Conference on Fluid Power and Mechatronics, Beijing-China, pp. 481-486, August 2011.

- [29] Starr, G., "Edge Following with a Puma 560 Manipulator using Val-II," Proceedings of the 1986 IEEE International Conference on Robotics and Automation, pp. 379- 383, April 1986.
- [30] Bossert, D., Ly, U., Vagners, J., "Experimental Evaluation of a Hybrid Position and Force Surface Following Algorithm for Unknown Surfaces," Proceedings of the 1996 IEEE International Conference on Robotics and Automation, Minneapolis-Minnesota, pp. 2252-2257, April 1996.
- [31] Kazanzides, P., Bradley, N. S., Wolovich, W. A., "Dual-Drive Force/Velocity Control: Implementation and Experimental Results," Proceedings of the 1989 IEEE International Conference on Robotics and Automation, Scottsdale-AZ, pp. 92-97, May 1989.
- [32] Yoskhihawa, T., Sudou, A., "Dynamic Hybrid Position/Force Control of Robot Manipulators – Online Estimation on Unknown Constraint," IEEE Transactions on Robotics and Automation, vol. 9, no. 2, pp. 220-226, 1993.
- [33] Whitcomb, L. L., Arimoto, S., Naniwa, T., Ozaki, F., "Adaptive Model-Based Hybrid Control of Geometrically Constrained Robot Arms," IEEE Transactions on Robotics and Automation, vol. 13, no. 1, pp. 105-116, 1997.
- [34] Novakovic, B. M., "Feedforward Neural Networks for Adaptive Nonlinear Robot Control," Proceedings of the 1994 IEEE/RSJ/GI International Conference on Intelligent Robots and Systems, Munich-Germany, pp. 486-493, September 1994.
- [35] Katic, D., Vukobratovic, M., "Learning Control Algorithms for Robot Contact Task Using Feedforward Neural Networks," Proceedings of the 1995 IEEE/RSJ International Conference on Intelligent Robots and Systems, Pittsburg-PA, pp. 522-527, August 1995.
- [36] Lin, C., Hsiao, Y., "Adaptive Feedforward Control for Disturbance Torque Rejection in Seeker Stabilizing Loop," IEEE Transactions on Control Systems Technology, vol. 9, no. 1, pp. 108-121, 2001.
- [37] Lanari, L., Wen, J. T., "Feedforward Calculation in Tracking Control of Flexible Robots," Proceedings of the 30<sup>th</sup> Conference on Decision and Control, Brighton-England, pp. 1403-1408, December 1991.

- [38] Flores, J., Tang, Y., Osorio, A., "Adaptive Feedforward Control and Disturbance Cancellation," Proceedings of the 32<sup>nd</sup> Conference on Decision and Control, San Antonio-Texas, pp. 2623-2628, December 1993.
- [39] Kelly, R., Saldago, R., "PD Control with Computed Feedforward of Robot Manipulators: A Design Procedure," IEEE Transactions on Robotics and Automation, vol. 10, no. 4, pp. 566-571, 1994.
- [40] Zaher, A., Zohdy, M., Areed, F., " Adaptive Feedforward Control of Processes with Parameters Uncertainty," 2003 IEEE 46<sup>th</sup> Midwest Symposium on Circuits and Systems, vol. 3, pp. 1034-1038, December 2003.
- [41] Shimada, A., Takeda, T., "Multirate Feedforward Control of Robot Manipulators," Proceedings of the 2007 IEEE/RSJ International Conference on Intelligent Robots and Systems, San Diego-CA-USA, pp. 4083-4088, November 2007.
- [42] Duan, S., Chen, L., Ma, Z., Chen, L., "Variable Structure Control with Feedforward Compensator for Robot Manipulators Subject to Load Uncertainties," 2011 11<sup>th</sup> International Conference on Control, Automation, Robotics and Vision, Singapore, pp. 2367-2372, December 2010.
- [43] Jatta, F., Adamini, R., Visioli, A., Legnani, G., "Hybrid Force/Velocity Contour Tracking: an Experimental Analysis of Friction Compensation Strategies," Proceedings of the 2002 IEEE International Conference on Robotics and Automation, Washington-DC, pp. 1723-1728, May 2002.